MEASUREMENT OF POLLUTANT EMISSIONS FROM AN AFTERBURNING TURBOJET ENGINE AT GROUND LEVEL
II. GASEOUS EMISSIONS

G. R. Lazalier and J. W. Gearhart

ARO, Inc.

August 1972

Approved for public release; distribution unlimited.

ENGINE TEST FACILITY
ARNOLD ENGINEERING DEVELOPMENT CENTER
AIR FORCE SYSTEMS COMMAND
ARNOLD AIR FORCE STATION, TENNESSEE

...F FORCE
...ARY
F40600-73-C-0004

NOTICES

When U. S. Government drawings specifications, or other data are used for any purpose other than a definitely related Government procurement operation, the Government thereby incurs no responsibility nor any obligation whatsoever, and the fact that the Government may have formulated, furnished, or in any way supplied the said drawings, specifications, or other data, is not to be regarded by implication or otherwise, or in any manner licensing the holder or any other person or corporation, or conveying any rights or permission to manufacture, use, or sell any patented invention that may in any way be related thereto.

Qualified users may obtain copies of this report from the Defense Documentation Center.

References to named commercial products in this report are not to be considered in any sense as an endorsement of the product by the United States Air Force or the Government.

MEASUREMENT OF POLLUTANT EMISSIONS FROM AN AFTERBURNING TURBOJET ENGINE AT GROUND LEVEL II. GASEOUS EMISSIONS

G. R. Lazalier and J. W. Gearhart
ARO, Inc.

FOREWORD

The test program reported herein was conducted at the request of the Air Force Aero Propulsion Laboratory (AFAPL), Air Force Systems Command (AFSC), Wright-Patterson Air Force Base, Ohio, under AFAPL Project Orders 71-7 and 72-9. The Program Element was 62203F, Project 3066, and Task 05. The AFAPL Project Engineer was Mr. K. N. Hopkins, and the AEDC Air Force Program Monitor was Mr. E. L. Hively. The test hardware, support hardware, test planning, and test procedures, exclusive of the J85-GE-5 turbojet engine and a mobile control van, were provided by AEDC. The turbojet engine and mobile control van were supplied by AFAPL.

The results of the test program were obtained by ARO, Inc. (a subsidiary of Sverdrup & Parcel and Associates, Inc.), contract operator of the Arnold Engineering Development Center (AEDC), AFSC, Arnold Air Force Station, Tennessee, under Contract F40600-73-C-0004. The test was conducted at the Ground Level Test Stand of the Engine Test Facility (ETF) during the period from June 22 through September 2, 1971, under ARO Project No. RW5239. The manuscript was submitted for publication on March 20, 1972.

This report presents the results from the second part of a two-part test program and describes a portable system for measuring gaseous emissions from afterburning turbojet engines. The results of the first part are presented in (AEDC-TR-72-64) which describes the techniques and results of measuring smoke emissions in accord with the Society of Automotive Engineers Aerospace Recommended Practice 1179.

This technical report has been reviewed and is approved.

EULES L. HIVELY
Research and Development
Division
Directorate of Technology

R. O. DIETZ
Acting Director
Directorate of Technology

ABSTRACT

The performance of a sampling and measurement system for the gaseous species of carbon monoxide (CO), carbon dioxide (CO_2), total hydrocarbons (C_xH_y), nitrogen dioxide (NO_2), and total oxides of nitrogen (NO_x) was demonstrated for engine power conditions from idle to maximum afterburning at ground level. Data were obtained, using a portable emissions measurement system developed at AEDC, at positions ranging from immediately at the nozzle exit to 96 ft aft of the nozzle exit plane. A J85-GE-5 engine was used to generate the gaseous emissions. Nondispersive infrared detectors were used for CO and CO_2 measurements; a flame ionization detector was used for C_xH_y measurements; and electrochemical devices operating on the fuel cell principle were used for NO_2 and NO_x measurements. The effects of inlet humidity and crosswind velocity on the quantity and distribution of gaseous species in the exhaust plume were determined.

CONTENTS

APPENDIXES

I. ILLUSTRATIONS

Figure

Figure Page

Figure Page

II. TABLES

NOMENCLATURE

A	Area
A/B	Afterburner
C	Concentration, ppmv or percent volume
EGT	Exhaust gas temperature, °R
M	Molecular weight

N	Rotational speed, percent of rated
P	Inlet air total pressure, psia
ppmv	Parts per million by volume
T	Inlet air total temperature, °F
W	Flow, lbm/hr
τ	Time, sec
ϕ	Relative humidity, percent

SUBSCRIPTS

a	Air
ab	Afterburner
e	Engine
f	Fuel
i	Index for annular area of exhaust nozzle
t	Total

SECTION I
INTRODUCTION

Noxious emissions from aircraft turbine engines have become increasingly important as the number, size, and combustion temperatures of engines have increased. Knowledge of the composition of the exhaust gas is essential to any effort undertaken to control or reduce the harmful emissions. Such knowledge can also be applied to the verification of models of combustion processes and to the determination of the results of experimental modifications to the engine.

Several methods for determination of exhaust gas composition are known. These techniques may be arbitrarily separated into three groups: wet-chemicals, dry-chemicals, and optical techniques. Sampling methods may be divided into continuous and batch sampling.

Wet-chemical techniques provide good accuracy in measurements but are usually cumbersome in that they require handling of liquid reagents with not infrequent replacement of the reagents. Dry-chemical techniques (i.e. electrochemical) are not as accurate as wet-chemical techniques but are usually fast, and the apparatus can be operated by semiskilled personnel. Optical techniques encompass a large variety of operating principles and may range from very complex to simple in concept. In general, nondispersive techniques are less complex than spectral techniques; however, nondispersive techniques suffer from contaminant (e.g. water vapor) interference effects.

Batch sampling may result in continued chemical activity in the stored sample gases. Large variations of the actual emissions with time (on the order of seconds) may result in erroneous characterization of engine emissions, depending on the particular level of the sample captured. Continuous sampling minimizes the time available for continued chemical interaction and reveals time variations in the data.

A program to develop a mobile, self-contained gaseous and solid particulate (Ref. 1) emissions measurement system for field use and to define the exhaust emissions field of a typical turbojet engine was conducted in the Engine Test Facility (ETF) at the Arnold Engineering Development Center (AEDC). The engine used during this investigation was a production J85-GE-5 engine supplied by the Air Force Aero Propulsion Laboratory (AFAPL). Testing was conducted at the Ground Level Test Stand of the ETF.

The results of the exhaust gas emissions measurement development effort are presented herein. A brief description is given of the emission measurement system which was utilized for sampling of the J85-GE-5 engine exhaust gases. The system made use of single-specie, dry-chemical or optical techniques, with continuous sampling and analysis procedures. Gaseous species measured were carbon monoxide, carbon dioxide, hydrocarbons, total oxides of nitrogen, and nitrogen dioxide.

Emissions data for the above species from the J85-GE-5 engine were obtained for distances of zero to 96 ft aft of the nozzle exit plane at engine power levels from idle to maximum afterburning. These data are presented and discussed as functions of both

power level and axial distance, as well as radial distance from the engine centerline, and represent the first systematic mapping of the gaseous emissions of a turbojet exhaust plume over this range of engine power.

SECTION II
APPARATUS

2.1 EMISSIONS MEASUREMENT SYSTEM

Five species were measured: hydrocarbons (C_xH_y), carbon monoxide (CO), carbon dioxide (CO_2), nitrogen dioxide (NO_2), and oxides of nitrogen (NO_x). A schematic of the measurement system is shown in Fig. 1 (Appendix I). The millivolt output of each instrument used for species concentration measurements was recorded on strip charts.

2.1.1 Hydrocarbons

Measurement of the hydrocarbons present in the exhaust products was made utilizing a Beckman Model 400 flame ionization detector (FID) shown schematically in Fig. 2. The FID operates by passing the sample gas through a very hot hydrogen-air flame resulting in a complex process of ionization of the hydrocarbon molecules which produces positive ions and electrons. The amount of ionization is determined by measuring the amount of electrical current passed through the ionized gas at a constant potential. The ionization current is then related to hydrocarbon concentration expressed as methane (CH_4) equivalent.

2.1.2 Carbon Monoxide and Carbon Dioxide

Beckman Model 315A nondispersive infrared (NDIR) instruments depicted schematically in Fig. 3 were used to measure the concentrations of carbon monoxide and carbon dioxide. Radiation was passed through a pair of gas-filled columns. One column was filled with a reference gas which has minimal absorption of energy at wavelengths absorbed by CO or CO_2; the other contained the sample gas. Because certain wavelengths of radiation are selectively absorbed by CO or CO_2, the differential amount of energy which passes through the columns yields information concerning the concentration of CO or CO_2 in the sample column. The difference in radiant energy passed through the columns is measured through absorption of the energy from each column in a fixed mass of the gas of interest (CO or CO_2). The fixed mass is contained in two cells which are connected by a flexible wall. Differences in the amount of energy absorbed result in a differential pressure across the wall with the subsequent deflection causing a change in capacitance of the detector. The change in capacitance is measured and displayed by the unit.

2.1.3 Nitrogen Dioxide and Oxides of Nitrogen

Electrochemical devices operating on the principle of fuel cells (Dynasciences Models NR-210 and NX-130) were used to measure the concentrations of NO_2 and NO_x. Details of the chemical processes are proprietary to the manufacturer. A representation of a typical sensor is shown in Fig. 4. The devices operate, in general, by selective passage through

a semi-permeable membrane and selective ionization of the species of interest (Ref. 2). Gas molecules which reach the surface of the sensor cause the following reactions (Ref. 2):

1. Change of ionic conductivity of the electrolyte,
2. Swelling of the electrolyte, and
3. Oxidation/reductions reactions involving the solid electrolyte and/or the metal film interface.

Each of these reactions can result in a change of current flow through the cell. These reactions are specific to various gas species.

2.1.4 Calibration of Gaseous Emissions Sensors

Calibrations of all systems were made by passing a nonparticipating carrier gas containing the gas of interest in varying concentrations through the instrument. Calibration of the FID was accomplished using methane (CH_4) in nitrogen. The NDIR's were calibrated using either CO or CO_2 in dry nitrogen. The NO_2 unit was calibrated using NO_2 in nitrogen, while both NO and NO_2 (separately) in nitrogen were used to calibrate the NO_x unit. Pre- and posttest calibrations consisted of checking the output of the units with the carrier gas alone (for zero calibration) and with the carrier gas containing a single concentration of the gas of interest (for upscale calibration).

2.2 GAS GENERATOR

The J85-GE-5 engine (Fig. 5) has an eight-stage, axial-flow compressor directly coupled to a two-stage turbine, a through-flow annular combustor, an afterburner, and a variable-area exhaust nozzle. Exhaust nozzle area is scheduled by power lever for nonafterburning operation. During afterburner operation, the nozzle is controlled to hold exhaust gas temperature constant (Fig. 6). The engine inlet diameter is approximately 15.4 in., and the overall length is approximately 108 in. Rated sea-level-static thrust is 2500 lbf at military power and 3850 lbf at maximum power (Ref. 3). Rated airflow is 44 lbm/sec at 16,500 rpm compressor rotational speed. Nominal values of several engine parameters for the power levels utilized in this investigation are presented in Table I (Appendix II) (Refs. 3 and 4).

The afterburner consists of a diffuser, a single V-gutter pilot burner which also acts as a flameholder, and a pilot burner fuel injection system. The pilot burner incorporates a spark plug igniter for afterburner ignition.

The integrated fuel system consists of main and afterburner fuel controls operated by the power lever. The main fuel control meters fuel as a function of compressor inlet total temperature, compressor discharge static pressure, engine rotor speed, and power lever angle.

2.3 INSTALLATION

The engine was mounted on a standard USAF flatbed trailer secured with cables. The trailer and engine were housed in an open-ended building. The installation is shown in Fig. 7. A bellmouth was attached to the inlet of the engine to provide uniform flow. A uniform low density screen provided protection from ingestion of foreign objects.

A trapezoidal concrete slab 100 ft in length was located aft of the engine exit plane. The width of the slab increased from 20 ft at the exit plane to 40 ft at the 100-ft location.

The exhaust gas sampling probe (Fig. 7c) was mounted on a movable cart and was capable of remote vertical straight line traverses of up to 8 ft. Axial and horizontal positions could be established with reference to the engine nozzle exit plane by utilization of premarked survey points on the concrete slab. The probe and a thermostatically controlled heated line (250°F) 50 ft in length were made of braided stainless steel with an interior coat of Teflon®. The probe was cooled or heated (depending on proximity to exhaust plane) by a circulating ethylene glycol mixture maintained at approximately 250°F. Sampling was accomplished both sub-isokinetically (at the nozzle exit) and super-isokinetically (far aft of the nozzle exit). Flow rates through the probe were always at least an order of magnitude greater than required by the measurement system.

2.4 INSTRUMENTATION

Instrumentation to provide definition of the operating conditions of the engine and the inlet environmental conditions was provided.

2.4.1 Engine Operating Parameters

Measurements of a minimal number of engine operating parameters were made to define engine operating conditions. Engine inlet and compressor discharge total pressure, engine rotational speed, engine inlet and turbine discharge total temperatures, and engine and afterburner fuel flows were measured using standard USAF supplied sensors. All data were manually recorded from the output of various standard gage displays.

2.4.2 Environmental Conditions

A continuous recording chart was used to record the output of a combination ambient temperature and relative humidity sensor. Atmospheric pressure measurements were obtained on a regular 2-hr schedule. Wind speed and direction were continuously recorded.

SECTION III
PROCEDURE

The J85-GE-5 engine was operated in the Ground Level Test Stand. Prior to engine start all data acquisition systems were conditioned and calibrated. Concentration data were recorded continuously, and data points were established after stabilization of all acquisition systems at the particular condition of interest. Data values for a given data point were averaged from strip chart traces over a 1-min time period.

Sample gases were drawn to a supply manifold (by a downstream diaphragm pump) from the sample probe through a 50-ft stainless steel line internally coated with Teflon which was heated to approximately 250°F to prevent condensation of water and hydrocarbons. Flow rates through the manifold were an order of magnitude or more greater than the totals required by the instruments. Residence times of the gases in the line were approximately 2.0 sec. Individual noncontaminating pumps were used to move sample gases from the sample manifold to the individual instruments for analysis (Fig. 1). Flow rates to individual instruments were set to the ranges specified by the manufacturer by use of throttling valves. Prior to testing, the entire system was purged using ambient air.

The J85-GE-5 engine is limited to 30-min operation at military (maximum nonafterburning) power and 5-min operation at maximum afterburning power (Ref. 3). These time limits were not exceeded during the test program.

Fuel conforming to MIL-T-5624G, Grade JP-4 (Ref. 5) was used throughout this investigation. The specified chemical composition of the fuel is presented in Table II. No chemical analysis of the fuel used was made; however, the fuel used was within specified limits for corrosion, heating values, distillation temperatures, and specific gravity.

Data were reduced by using millivolt output readings from the various instruments in conjunction with previously defined calibration curves expressed as concentration in terms of millivolt outputs.

SECTION IV
RESULTS AND DISCUSSIONS

The objective of this test was to demonstrate the performance of a gaseous pollutant measurement system in the exhaust plume of an afterburning turbojet engine operating at ground level. A J85-GE-5 engine was used to generate the exhaust gases. Data were obtained at several engine power levels from idle to maximum afterburning and at several axial and radial positions (in the vertical plane only). Power conditions were defined in terms of rated military thrust of the J85-GE-5 engine (Table I) as determined from engine specifications (Ref. 3) for speed and fuel flow. Inlet temperature, pressure, and humidity ranged from 69 to 101°F, 14.18 to 14.28 psia, and 50 to 100 percent, respectively.

4.1 SAMPLING SYSTEM PERFORMANCE

The performance of the sampling system is described in terms of the accuracy, resolution, and response rate of the individual instruments and the instruments coupled with the sampling probe and transfer line. Data are presented detailing the measured variations in concentration levels encountered during actual operation with the turbojet engine at constant power level and at the same spatial location. The effects of sampling probe and transfer line designs are discussed.

4.1.1 Uncertainty, Variations, and Response Rate

The steady-state uncertainties of the gaseous emissions measuring system are presented in Table III. Resolution of each instrument to the isolated specie of interest was within the width of the pen used on the direct-reading analog chart recorder.

Typical variations of data measurements obtained for all species during operation 4 ft aft (over a 1-min time span) of the nozzle exhaust of the J85-GE-5 at cruise power are presented in Table IV. Data variation is a function of the combination of instrument and recorder resolution, gas generator emissions stability, and variations induced by the sampling systems. These variations ranged from ±0.4 percent (CO_2) to ±5.5 percent (C_xH_y) of the mean levels for the data point described in Table IV. In general, variations for all data obtained tended to approximate those detailed in Table IV, with total hydrocarbons exhibiting the widest resolution band.

The times for each instrument to respond to 90 percent of the steady-state reading for the isolated species of interest are presented in Table V. The times ranged from a minimum of 3 sec for carbon monoxide and carbon dioxide to a maximum of 220 sec for nitrogen dioxide. Also presented in Table V are the estimated response times of the entire system. The difference in response times of the system and the individual instruments can be attributed to the sum of (1) transport times from the probe to the instrument (2.0 sec in the transfer line plus 2 to 5 sec in the internal plumbing of the instrument system) and (2) the need to purge the system of gases from the prior operating point (approximately two to three gas changes). Response times of nitrogen dioxide and total oxides of nitrogen were essentially identical for the entire system compared with the instrument alone.

4.1.2 Precision of System Measurements Including the Turbojet Engine Emissions Variations

Data obtained at 16 ft aft of the engine exhaust for military and maximum afterburning power are presented in Fig. 8 as functions of test number (day) to demonstrate the repeatability of the entire system. Data bands for carbon dioxide and total oxides of nitrogen exhibited minimal variations from the mean. The maximum percentage deviation of carbon dioxide was -9.4 percent (-0.094 percentage points at a mean level of 1.00 percent), while the maximum deviation of total oxides of nitrogen was +13 percent (+1.5 ppmv at a mean level of 11.1 ppmv). Deviations of up to +46 percent and +25 percent were noted for hydrocarbons and carbon monoxide, respectively (+59 ppmv at a mean level of 222 ppmv for C_xH_y and +8.6 ppmv at a mean level of 18.9 ppmv for CO). Variations shown in Fig. 8 include all system variables, including the actual variation in emissions from the engine.

4.1.3 Sample Probe and Transfer Line Design Considerations

The use of a sample probe and transfer line is necessary to allow maintenance of the operating environment required by the gaseous emissions measuring instruments. Use of these elements introduces several factors which may influence the composition of the gaseous sample delivered to the measuring instruments.

The volumetric flow rate at the entrance to the probe determines the nature of the flow phenomena which occur to adjust the external flow to the conditions internal to the probe. Sampling can be accomplished sub-isokinetically, isokinetically, or super-isokinetically and can result in the formation of deceleration shock waves (in

supersonic external flow) and/or non-shock deceleration zones (for sub-isokinetic) or acceleration zones (for super-isokinetic) with attendant different temperature profiles. No effort to control probe inlet conditions, with respect to isokinetic considerations, was made for the results detailed herein. Flow rate through the sampling probe was maintained at approximately 1.0 ft^3/min in order to hold constant the time spent by the sample in the transfer line at approximately 2.0 sec.

The temperature of the transfer line and sampling probe must be held high enough to prevent condensation of water and low enough to prevent continued reaction of the various constituents of the sample gas. Recent investigations indicate the lower temperature limit for quantitative conversion of NO_2 to NO in the presence of stainless steel to be 320°F (Ref. 6). The sample transfer line used in this investigation was maintained at approximately 250°F throughout its length.

4.2 EFFECTS OF RAIN AND HUMIDITY ON POLLUTANT EMISSION CHARACTERISTICS

Pollutant emission data were obtained at several power levels with inlet environmental humidity conditions ranging from 50 percent relative humidity to heavy rain (no drop ingestion at the inlet). Data obtained for these environmental conditions are presented in Fig. 9. No consistent trend of pollutant levels with environmental conditions could be detected for any species over the range of conditions tested. For any particular inlet environment at a selected power level, the data obtained at other environmental conditions (on different days) are within the data band. Examples are afforded by carbon monoxide (Fig. 9a) with heavy rain at minimum afterburning, hydrocarbons emissions (Fig. 9c) with 70-percent relative humidity at cruise and military, and nitrogen dioxide emissions (Fig. 9e) with 50-percent relative humidity at cruise, military, and mid and maximum afterburning.

4.3 EFFECTS OF WIND DISTRIBUTIONS

The maximum sustained crosswind component experienced was 7 miles per hour, while the average was 3 or less. Centerline jet velocities were estimated to be from 200 to 1000 ft/sec at the 16-ft station (Ref. 3), depending on power level. Estimated plume centerline deflection at maximum afterburning resulting from crosswinds was less than 1-1/2 in. for the maximum crosswind condition at 16 ft aft of the nozzle (Fig. 10).

Radial distributions of pollutant concentrations (taken in the vertical plane) at military power 16 ft aft of the nozzle exit plane with varied crosswind conditions are presented in Fig. 11 for carbon monoxide, carbon dioxide, and hydrocarbons. No significant effects of crosswind on radial distributions were observed.

4.4 CENTERLINE POLLUTION EMISSION CHARACTERISTICS

4.4.1 Effects of Power Level on Pollutant Levels

Data were taken at power levels corresponding to idle, cruise, military, and various afterburner levels (see Table 1). Pollutant concentrations on the engine centerline at the

nozzle exit and 16 ft aft of the nozzle exit are presented in Fig. 12 as functions of nominal engine power level. The inviscid core of the exhaust plume extended less than 16 ft at all power conditions tested. Therefore, the level changes documented in the following paragraphs are largely the result of entrainment of ambient air with the consequent dilution of the concentration levels. At the higher afterburning powers a portion of the changes in hydrocarbon and carbon dioxide concentration levels is the result of continued reactions within the inviscid core.

Carbon monoxide levels (Fig. 12a) were maximal at idle and minimum afterburning power (as shown by the data obtained at 16 ft) for all axial positions investigated except at the nozzle exit plane. The reversal in trend of carbon monoxide emissions with engine power (nozzle exit values compared with values at all downstream positions) probably results from continued reaction at the high temperatures associated with the higher power levels of afterburning.

Carbon dioxide emissions (Fig. 12b) increased monotonically with increasing power level at all axial positions investigated. The maximum level observed on the engine centerline was 9.1 percent at maximum afterburning power at the nozzle exit.

Emissions of hydrocarbons (Fig. 12c) ranged from ~10 ppmv at 16 ft with maximum afterburner to 6600 ppmv at the nozzle exit with mid-afterburner power. Levels tended to be minimal at military and maximum afterburning power levels.

Emissions of total oxides of nitrogen (Fig. 12d) ranged upward to 340 ppmv at the nozzle exit with mid-afterburning power. A reversal in trend at afterburning conditions was observed at the nozzle exit as compared with the 16-ft location. This reversal is believed to be caused by continued reaction of the gaseous exhaust at the high temperatures associated with afterburning operation.

Nitrogen dioxide (Fig. 12e) emissions, which account for a significant portion of the total oxides of nitrogen levels, tended to increase with increasing power. The maximum value observed was 56 ppmv at the nozzle exit with minimum afterburning power.

4.4.2 Effects of Axial Distance on Pollutant Levels

Data were taken from 0 to 96 ft aft of the engine nozzle exit plane. The concentrations of the various pollutants as functions of axial distance are presented in Figs. 13 through 16 for power levels of cruise, military, and minimum and maximum afterburning.

With the exception of emissions measured interior to the inviscid core, which extended from approximately 3 to 6 ft (2.2 to 6.5 nozzle diameters) aft, concentrations of all pollutant species decreased with increasing axial distance aft of the nozzle exit plane. Levels of all pollutant species decreased by an order of magnitude or more from the nozzle exit to 96 ft aft. At maximum afterburning, levels of hydrocarbons observed at the exit of the nozzle were approximately an order of magnitude greater than those observed at the 4-ft-aft axial location.

4.5 RADIAL DISTRIBUTION OF POLLUTANTS

Radial distributions of pollutant concentrations at various power levels were determined at 0, 4, 8, and 16 ft aft of the engine nozzle exit plane. Data were obtained at idle power only at the nozzle exit plane because the relatively low velocity jet at idle power decayed rapidly.

4.5.1 Effects of Power Level on Radial Distributions

Distributions of pollutant concentrations obtained at the engine nozzle exit plane are presented as functions of radial location in Fig. 17. Distributions obtained at nonafterburning power levels tended to be considerably more uniform than those obtained at afterburning power levels. Pronounced irregularities can be discerned for the afterburning power profiles. Operating experience, in the form of repeated profile data, revealed variations in the output of the engine.

4.5.2 Effects of Axial Distance on Radial Distributions

Distributions of pollutant concentrations at distances from 0 to 16 ft aft of the engine nozzle exit plane are presented as functions of radial location and engine power in Figs. 18 and 19.

At military power (Fig. 18), all species measured were maximum at the nozzle exit station except for the centerline value of carbon monoxide emission (Fig. 18a), which was less at the exit station than at 4 ft aft as a result of a depression in the distribution profile. Hydrocarbon profiles were erratic at the nozzle exit plane and at the 4-ft station; however, at the 8- and 16-ft stations, the profiles measured were uniform. Concentration profiles of oxides of nitrogen (both NO_x and NO_2) were regular at all measurement stations.

At maximum afterburning power (Fig. 19), concentrations of all species were maximum at the nozzle exit station. Profiles of carbon monoxide and carbon dioxide contained depressions near the engine centerline. Levels of hydrocarbons were on the order of 100 ppmv at all axial stations except at the nozzle exit plane where a level of ~1250 ppmv was measured. Because of the continued reactions at afterburning power levels, downstream measurements of pollutant emissions are essential to adequately define interaction of the emission characteristics of engines and the atmosphere in the near-field.

4.6 RATIO OF CONCENTRATIONS OF NITROGEN DIOXIDE TO TOTAL OXIDES OF NITROGEN CONCENTRATIONS

Combustion of petroleum-based fuels such as JP-4 results in the formation of several oxides of nitrogen. Several studies (Refs. 7 and 8) have indicated that the initial product formed is largely nitric oxide (NO) at or near the flame source. It has also been found that the conversion of NO emitted to NO_2 is expected to occur on a scale of hours after mixing with the atmosphere for ambient temperatures and pressures at near standard sea level days. The centerline concentration at the nozzle exit of the ratio of NO_2 to that of total oxides of nitrogen (NO_x) as a function of engine power level is presented

in Fig. 20. Data from Figs. 13 through 17 were used to determine the ratios. Values ranged between 0.3 and 0.4 for idle and minimum and maximum afterburning and between 0.5 and 0.63 for cruise and military power levels. No dependence of the ratio of NO_2 to NO_x on axial distance could be confirmed.

4.7 COMBUSTION VARIATION AT AFTERBURNING POWER LEVELS

During operation at afterburning power levels, a cyclical variation in the combustion process was noted. The variation was noted on approximately 50 percent of the afterburning data points at the nozzle exit station and was greatest at maximum afterburning power. Presented in Fig. 21 are typical time histories of concentrations of the five species being measured. A direct correlation in the variations of the concentration level of each specie is apparent at a frequency of approximately 0.055 Hz (~3.3/min). Both carbon monoxide and hydrocarbons peak at the same time that carbon dioxide minimizes indicating a direct relation with the combustion process. The response times of the sensors used to determine oxides of nitrogen (NO_x and NO_2) are sufficiently slow to make a direct time correlation questionable. However, examination of these traces indicates a variation in level with the same frequency as for the other species.

A second slower variation of parameters may be noted over an approximately 3-min time span. This variation was typical of the stabilization time of the engine whenever it was changed from one power setting to another. Prior to the establishment of maximum afterburning power shown in Fig. 20, the engine was operating in a steady-state mode at idle power.

The presence of large variations (up to 50 percent for hydrocarbons) in pollutant emission levels with time for some afterburning power levels makes a continuous sampling technique desirable. If single point sample bottle techniques, lasting approximately 2 to 3 sec, had been used, considerable error could have been introduced into the data recorded, depending on the exact time of sample acquisition.

4.8 MASS RATE EMISSIONS OF POLLUTANTS

Concentration of emissions by volume, as presented in previous sections of this report, provides a means of studying the effects of various external parameters on engine emissions. However, comparison of emissions from different engines is often accomplished using figures of merit derived from mass rate emissions. Mass rate emissions and two figures of merit (lbm pollutant/lbm fuel; and lbm/pollutant/hr/lbf thrust) for carbon monoxide, carbon dioxide, total oxides of nitrogen, nitrogen dioxide, and hydrocarbons expressed as methane (CH_4) are presented in Table VI for idle, cruise, military power, and minimum, mid, and maximum afterburning.

The technique used to calculate the emission rates is presented as follows:

$$\text{Emission rate (lbm/sec)} = \sum_{1}^{9} C_{x_i}\left(\frac{M_x}{M_e}\right)(W_a + W_{f_t})\,(A_i/A_t) \times 10^{-6}$$

where

C_x = concentration of species x, ppmv

M_x = molecular weight of species x

M_e = molecular weight of exhaust gas

$= 21.84 + C_{CO_2} \times 44 \times 10^{-6} + [0.22 - (C_{CO_2} \times 10^{-6})] \times 32$

W_a = airflow lbm/sec

W_{f_t} = total fuel flow lbm/sec

A_i = area associated with an individual measurement

A_t = total nozzle area

Calculations of total oxides of nitrogen (NO_x) emission rates were made by assuming that the NO_x emissions were comprised of only nitric oxide (NO) emissions (which were not explicitly measured) and nitrogen dioxide (NO_2) emissions (which were explicitly measured). The required values for NO_x molecular weights were calculated as follows:

$$C_{NO} + C_{NO_2} = C_{NO_x} \qquad \text{(volumetric balance)}$$

$$C_{NO} \frac{M_{NO}}{M_{ex}} (W_a + W_{f_t}) + C_{NO_2} \frac{M_{NO_2}}{M_{ex}} (W_a + W_{f_t}) = C_{NO_x} \frac{M_{NO_x}}{M_{ex}} (W_a + W_{f_t})$$

(mass balance)

Therefore:
$$M_{NO_x} = M_{NO} + \frac{C_{NO_2}}{C_{NO_x}} (M_{NO_2} - M_{NO})$$

4.8.1 Nonafterburning Emission Rates

Absolute emission rates of carbon dioxide, carbon monoxide, and nitrogen dioxide increased with power level from idle to military power. The absolute emission rate of total hydrocarbons decreased over the same power range.

The mass emissions per mass of fuel utilized decreased for carbon monoxide and total hydrocarbons over the idle to military power range while nitrogen dioxide emissions per mass of fuel increased from idle to cruise power and decreased slightly (~2 percent) at military power. The mass emission of carbon dioxide increased from 2.82 at idle power to 3.65 at cruise power and decreased to 3.54 at military power, indicating minimal combustion efficiency at idle power. The theoretical value for carbon dioxide product per mass of fuel for complete combustion of a fuel similar to JP-4 (assumed hydrogen: carbon ratio of 1.9) such as C_9H_{17} is approximately 3.15. The apparent upward bias in the mass emission rates per mass of fuel could have resulted from either a systematic bias in the individual values used for profile determination or from the simplified technique used to integrate over the nozzle exit area. Because only nine values, constituting one diametral profile, were used to calculate the mass emission rates, the probable cause of the bias is inaccuracies in the integration technique.

Mass emission rates per unit of thrust produced by the engine decreased with increasing power level for all species presented in Table VI except carbon dioxide.

4.8.2 Afterburning Emission Rates

Absolute emission rates of carbon dioxide increased with increasing power level during afterburning operation. Emission rates of total hydrocarbons decreased with increasing power during afterburning operation. Nitrogen dioxide and carbon monoxide emission rates decreased from minimum to mid-afterburning and increased at maximum afterburning.

Emissions per mass of fuel of carbon monoxide, total hydrocarbons, and nitrogen dioxide decreased with increasing power level. The ratio of carbon dioxide emissions to the mass of fuel utilized was almost constant at minimum and mid-afterburning power (3.25 and 3.36, respectively) and decreased sharply to 3.02 at maximum afterburning power.

Mass emission rates per unit of thrust produced by the engine decreased with increasing power level for all species presented in Table VI, except carbon dioxide.

4.9 OPERATIONAL EXPERIENCE

The gaseous emissions measurement techniques developed in the investigation reported herein were optimized for a mobile unit which could be operated by non-engineering personnel. The capability to determine the chemical composition of two multi-component species (hydrocarbons and total oxides of nitrogen) was not provided because complex, difficult-to-operate instruments (spectrographic or equivalent) are required for such determination. The constituent make-up of the two species is of importance because of the role hydrocarbons and total oxides of nitrogen assume in the production of photo-chemical smog (Ref. 7). Additionally, certain hydrocarbon compounds, e.g. the aldehydes, are important in odor formulation while others may be carcinogenic (Ref. 9). The observed change in the ratio of concentrations of nitrogen dioxide (NO_2) to concentrations of total oxides (NO_x) of nitrogen with power level indicates the existence of a chemical reaction involving these compounds. Data obtained from this program were not sufficient to establish either the nature of the reaction or the participating species.

Two significant technical accomplishments were realized during this program: (1) At the time the tests were made, the program provided the first set of comprehensive and systematic exhaust plume emissions data obtained from a turbojet engine in the afterburning mode. Documentation of the effects of exhaust plume dilution during normal ground operations was made over the entire range of engine power conditions for the J85-GE-5 test vehicle. (2) The presence of large variations with time (~3.3/min) of the exhaust emission concentrations of several species (notably, CO, CO_2, and C_xH_y) at afterburning power levels was discovered. Additional testing, including sampling internal to the afterburner, is required to determine the causes of such variations.

Overall operational experience with the gaseous emissions measurement system was good. However, response and stabilization times of some instruments (particularly the NO_x and NO_2 units) approached 5 min, which was the operational time limit at maximum afterburning power for the J85-GE-5 engine. The development of instrumentation for all species which satisfy not only the mobility and complexity-of-operation criteria but also a shorter (~0.5 min) maximum response time will aid in the rapid acquisition of data.

For approximately 25 of 75 data points taken at distances from 8 to 16 ft aft of the engine nozzle exit plane, indicated values of NO_2 concentration exceeded the indicated values of NO_x concentration. If it is assumed that, at these axial stations, the NO_x concentration consisted totally of NO_2, these measurements would seem inconsistent. However, for 23 of the 25 data points, the NO_2 and NO_x measurements were consistent within the combined measurement uncertainties presented in Table III. The measurements obtained during the remaining two data points were less than 1 ppmv outside the combined measurement uncertainty bands. Additionally, on approximately 5 of 62 data points taken at the nozzle exit plane, the indicated values of NO_2 concentration exceeded the indicated NO_x concentration. Two of these data points were consistent within the combined measurement uncertainties; the remaining three points were substantially outside the uncertainty bands. A possible explanation of this apparent discrepancy is that the electrochemical measurement devices may have been "poisoned" by excessive hydrocarbons, in the form of fuel droplets.

SECTION V
SUMMARY OF RESULTS

The performance characteristics of a measurement system to measure emissions of carbon monoxide, carbon dioxide, total hydrocarbons, nitrogen dioxide, and total oxides of nitrogen were determined. The emission characteristics and the distribution of the above species in the exhaust plume of a J85-GE-5 turbojet engine operating at ground level were determined. The significant results are as follows:

5.1 EMISSIONS MEASUREMENT SYSTEM PERFORMANCE

1. A mobile system to continuously acquire and analyze concentrations of carbon monoxide, carbon dioxide, total hydrocarbons, total oxides of nitrogen, and nitrogen dioxide in the exhaust of a turbojet/fan engine was developed, and its performance was demonstrated using a J85-GE-5 engine as an exhaust gas generator.

2. Concentrations of carbon monoxide over the range from 25 to 2500 ppmv were measured with precisions of ±1.65 to ±16.5 ppmv. Concentrations of carbon dioxide over the range from 0.3 to 9.0 percent were measured with precisions of ±0.022 to ±0.11 percentage points. Precisions of measurements of total hydrocarbons over the range from 20 to 4500 ppmv concentration were ±0.43 to ±34.4 ppmv. Total oxides of nitrogen concentrations over the range from 2 to 340 ppmv were measured with precisions of ±0.35 to ±1.05 ppmv. Nitrogen dioxide concentrations over the range from 2 to 60 ppmv were measured with precisions of ±0.175 to ±0.35 ppmv.

3. Concentrations of carbon monoxide over the range from 25 to 2500 ppmv were measured with uncertainties of ±12 to ±120 ppmv. Concentrations of carbon dioxide over the range from 0.3 to 9.0 percent were measured with uncertainties of ±0.16 to 0.80 percentage points. Uncertainties of

measurements of total hydrocarbons over the range from 20 to 4500 ppmv concentration were ±3.8 to 301 ppmv. Total oxides of nitrogen concentrations over the range from 2 to 340 ppmv were measured with uncertainties from ±3.6 to ±10.7 ppmv. Nitrogen dioxide concentrations over the range from 2 to 60 ppmv were measured with uncertainties of ±3.05 to 6.1 ppmv.

4. The times required for attainment of 90 percent of the steady-state value for each species after a step change in emissions concentration levels were as follows: carbon monoxide, 10 sec; carbon dioxide, 10 sec; hydrocarbons, 15 sec; oxides of nitrogen, 206 sec; and nitrogen dioxide, 226 sec. Residence time of the gas sample in the transfer line was approximately 2.0 sec. From two to three gas changes were required to purge the system of previously acquired gases.

5. The mobile sampling probe was either cooled to permit sampling at exhaust gas temperatures up to 3300°R (near the engine exit) or heated when located near the boundaries of the exhaust plume (where mixing of ambient air had cooled the exhaust gases) by a circulating mixture of ethylene glycol and water. Condensation of water in the sampling probe and transfer line was prevented by maintaining these elements at a controlled temperature (~250°F).

6. The operational suitability of the system was demonstrated by continued use over a time period of several months with only routine maintenance, in a variety of environmental conditions.

5.2 ENGINE EMISSIONS CHARACTERISTICS

1. Carbon monoxide emission concentrations tended to be maximal at idle power and minimum afterburning at all axial positions except at the nozzle exit. The absolute emission rate of carbon monoxide increased with increasing power during nonafterburning power and reached a maximum at minimum afterburning power. Levels at mid and maximum afterburning power were approximately twice those at military power.

2. Carbon dioxide emission concentrations and absolute emissions increased continuously with increasing power level.

3. Nitrogen dioxide emission concentrations and absolute emissions increased to a maximum at minimum afterburning and decreased at maximum afterburning to levels near the military levels.

4. Hydrocarbons emission concentrations maximized at minimum afterburning for all axial positions except at the nozzle exit where the maximum occurred at maximum afterburning. Absolute emissions decreased with increasing power during nonafterburning operation, increased to maximum at

minimum afterburning, and decreased at maximum afterburning to a level approximately twice that at military.

5. Total oxides of nitrogen emission concentrations maximized at minimum afterburning for all axial positions except at the nozzle exit where the maximum occurred at mid-afterburning.

6. Emissions per mass of fuel were minimum at maximum afterburning power for carbon monoxide and total hydrocarbons. Emissions of nitrogen dioxide and carbon dioxide per mass of fuel were minimum at idle power.

7. Emissions per unit of thrust were minimal at maximum afterburning power for carbon monoxide, nitrogen dioxide, and total hydrocarbons.

8. Centerline concentrations of all species decreased with increasing axial distance except for carbon monoxide at military power within the inviscid core.

9. Pronounced cyclical variations (on the order of 3/min; up to 50 percent for hydrocarbons) in gaseous emissions concentrations were noted at afterburning power. This phenomenon makes it desirable that continuous sampling be used in preference to batch sampling.

10. A significant change in the ratio of NO_2 to NO_x on the engine centerline at the nozzle exit was noted with engine power level. The ratio varied from approximately 0.3 at idle and minimum and maximum afterburning to 0.6 at cruise and military power levels.

11. Rain and relative humidity had no discernible influence on emissions concentrations.

REFERENCES

1. Gearhart, J. W. and Benek, J. A. "Measurement of Pollutant Emissions from an Afterburning Turbojet Engine at Ground Level, I. Particulate Emissions." AEDC-TR-72-64, June 1972.

2. Brown, V. and Tamstorf. "A New all Solid State Approach to Gaseous Pollutant Detection." AIAA Paper No. 71-114, Presented at the Joint Conference on Sensing on Environmental Pollutants, November 1971.

3. General Electric Company. "Model Specification E1024-B, Engine Aircraft, Turbojet J85-GE-5." June 30, 1960.

4. Faehl, K. C., Turner, E. E., and Kistler, S. M. "Afterburner Altitude Characteristics and General Performance of the J85-GE-5 Turbojet Engine, Appendix B, Tabulated Data." AEDC-TN-61-57 (AD257724), June 1961.

5. "Turbine Fuel, Aviation Grades JP-4 and JP-5." Military Specification MIL-T-5624G, November 1965.

6. Hodgeson, J. A., Bell, J. P., Rehme, K. A., Krost, K. J., and Stevens, R. K. "Application of a Chemiluminescence Detector for the Measurement of Total Oxides of Nitrogen and Ammonia in the Atmosphere." AIAA Paper No. 71-1067, Presented at the Joint Conference on Sensing of Environmental Pollutants, November 1971.

7. Sawyer, R. F., Teixeira, D. P., and Starkman, E. S. "Air Pollution Characteristics of Gas Turbine Engines." Transactions of the ASME, Journal of Engineering for Power, October 1969.

8. Smith, D. S., Sawyer, R. F., and Starkman, E. S. "Oxides of Nitrogen from Gas Turbines." Journal of the Air Pollution Control Association, Vol. 18, No. 1, January 1968.

9. Blaunstein, R. P. and Christophorou, L. G. "Electron Attachment by Organic Molecules." ORNL-TM-2216, 1968b.

APPENDIXES

I. ILLUSTRATIONS
II. TABLES

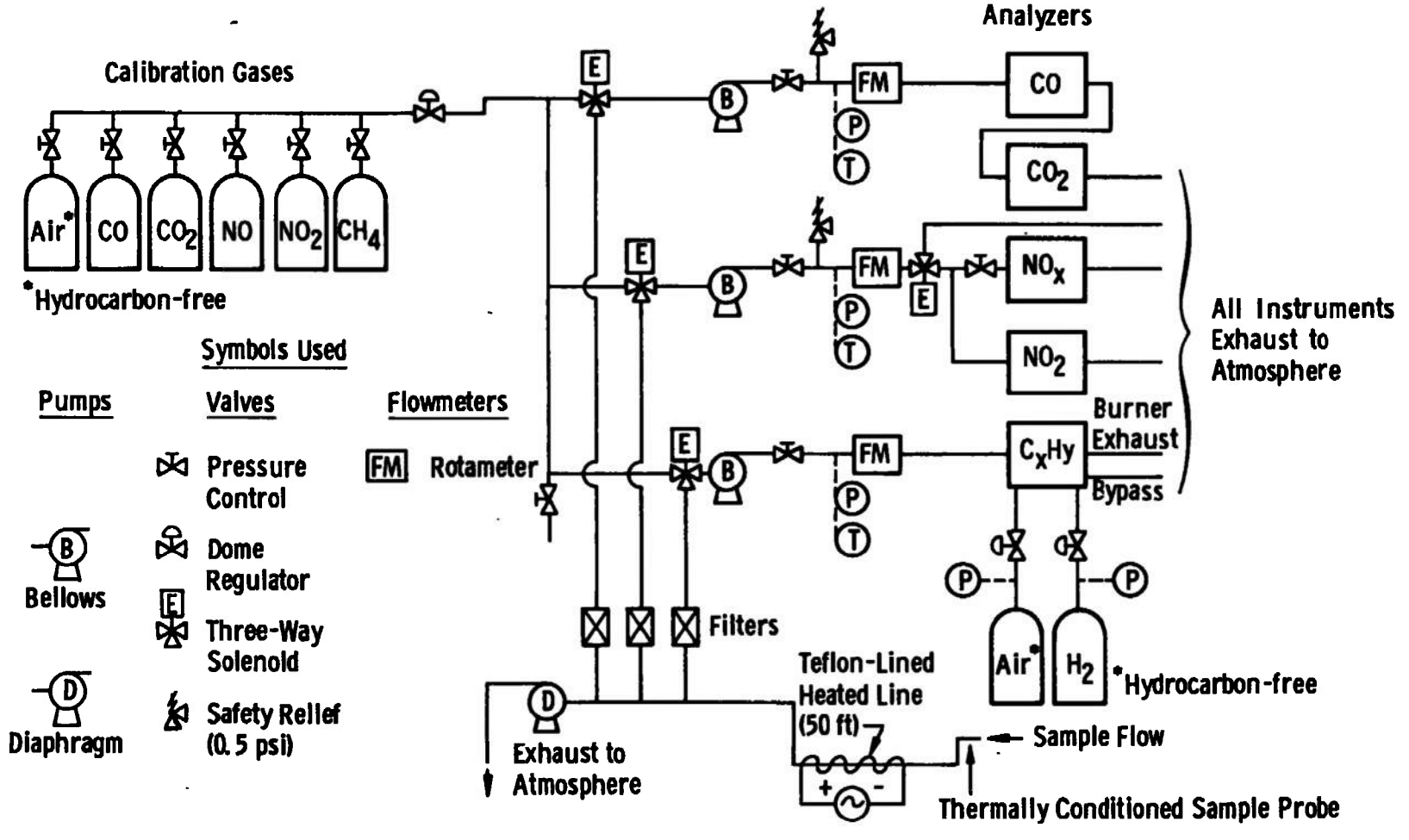

Fig. 1 Analysis System Schematic

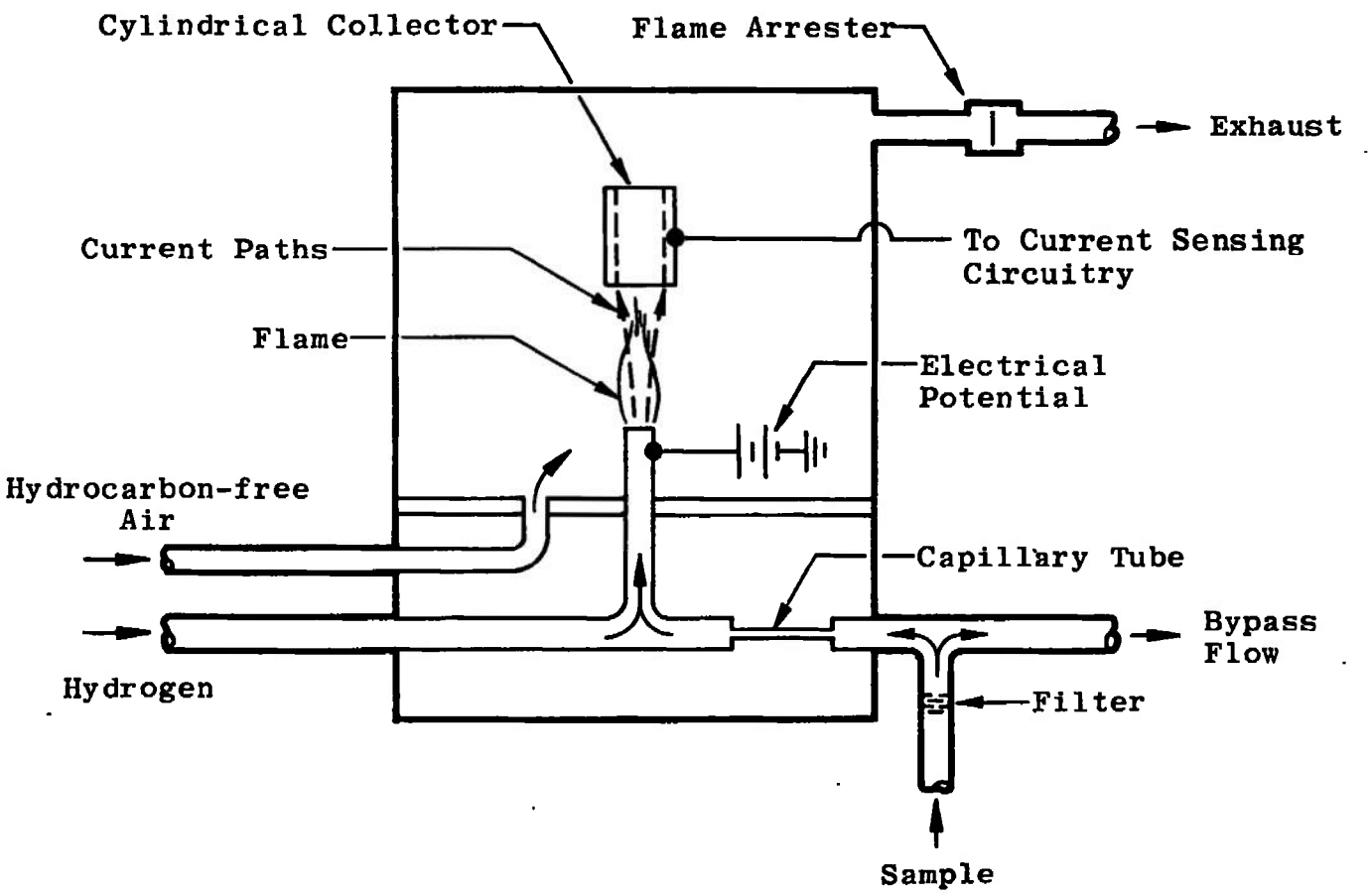

Fig. 2 Flame Ionization Detector Schematic

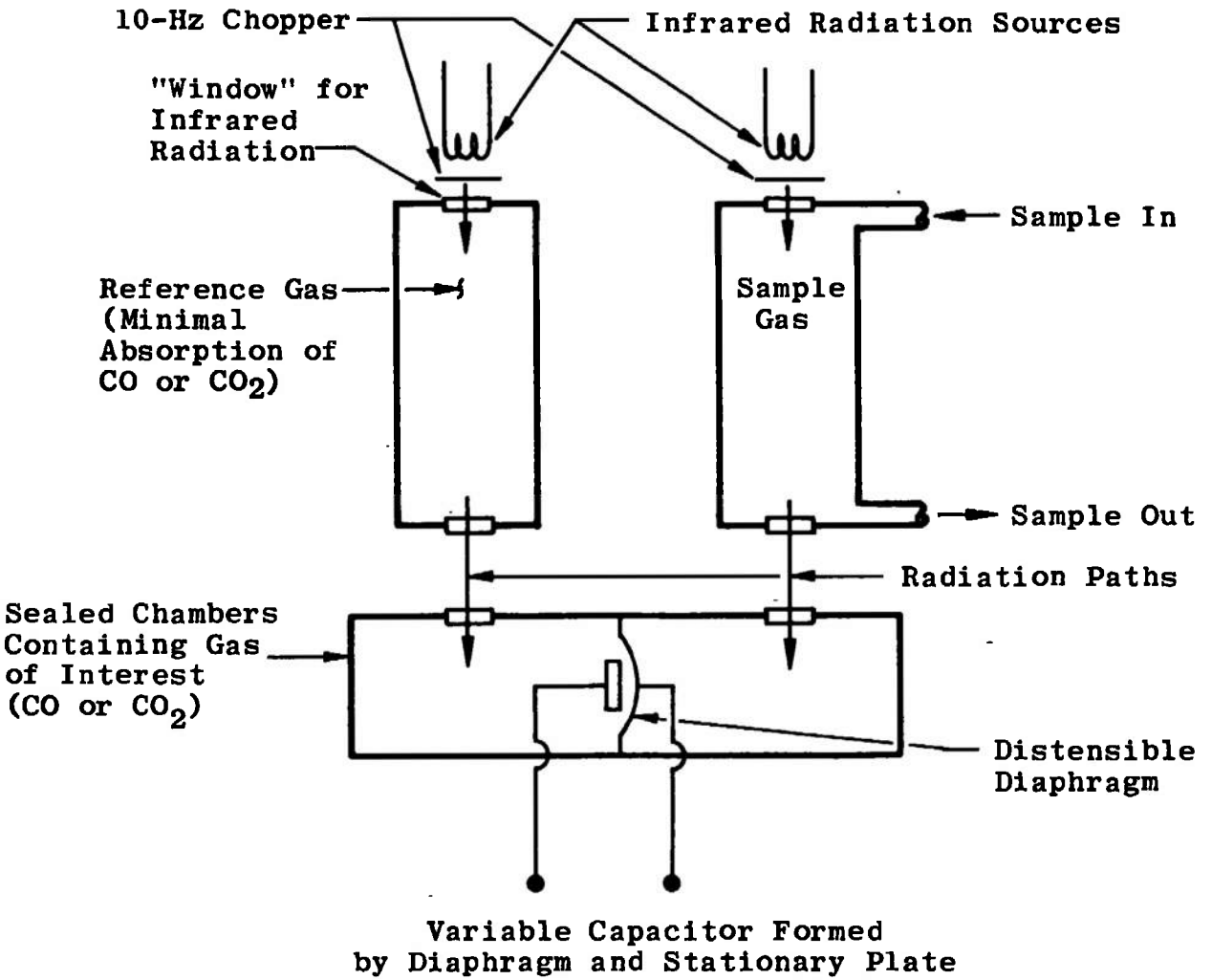

Fig. 3 Nondispersive Infrared Detector Schematic

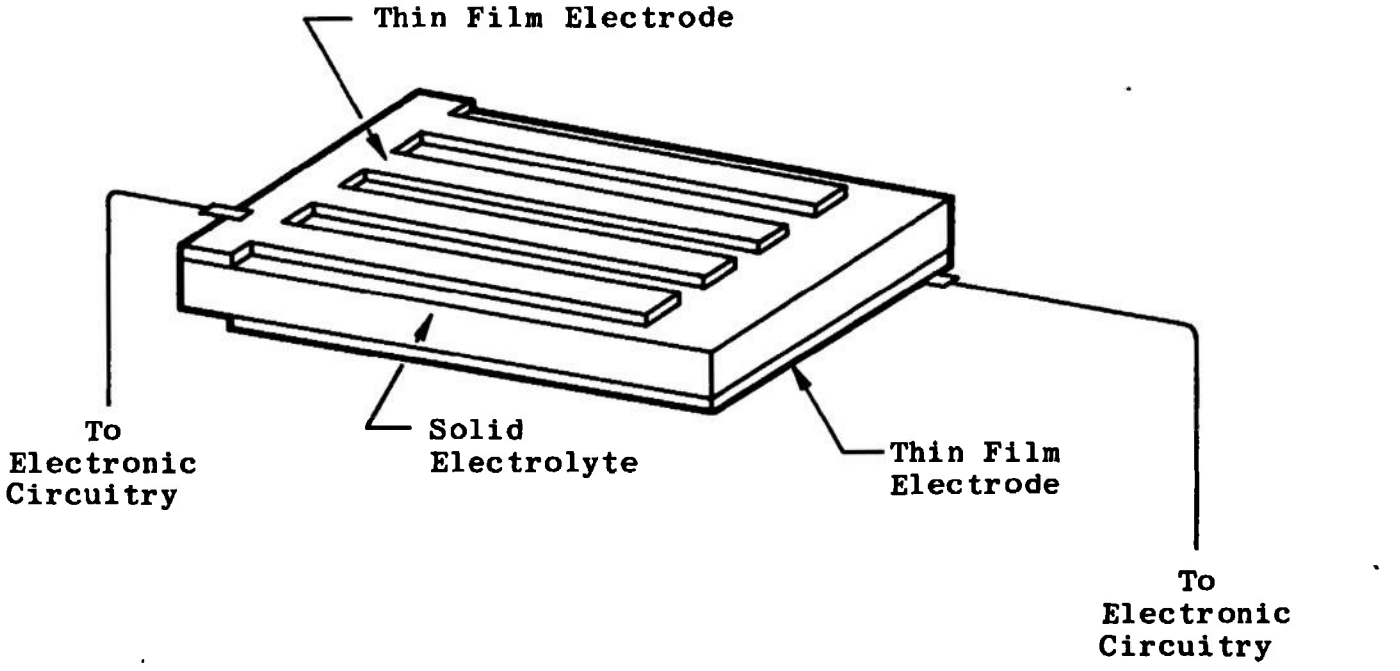

Fig. 4 Electro-Chemical Device Schematic

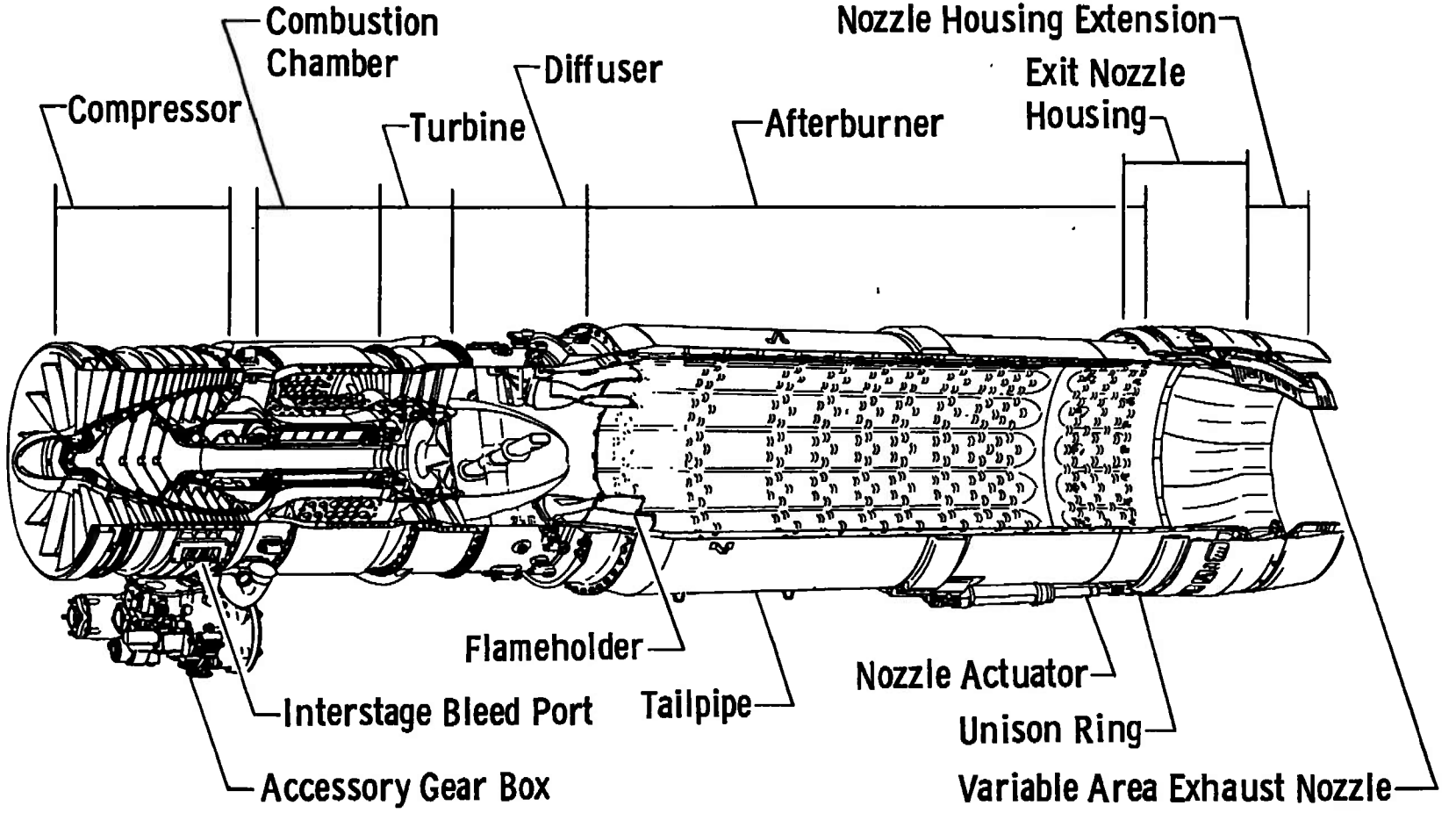

a. Cutaway Schematic

Fig. 5 J85-GE-5 Turbojet Engine

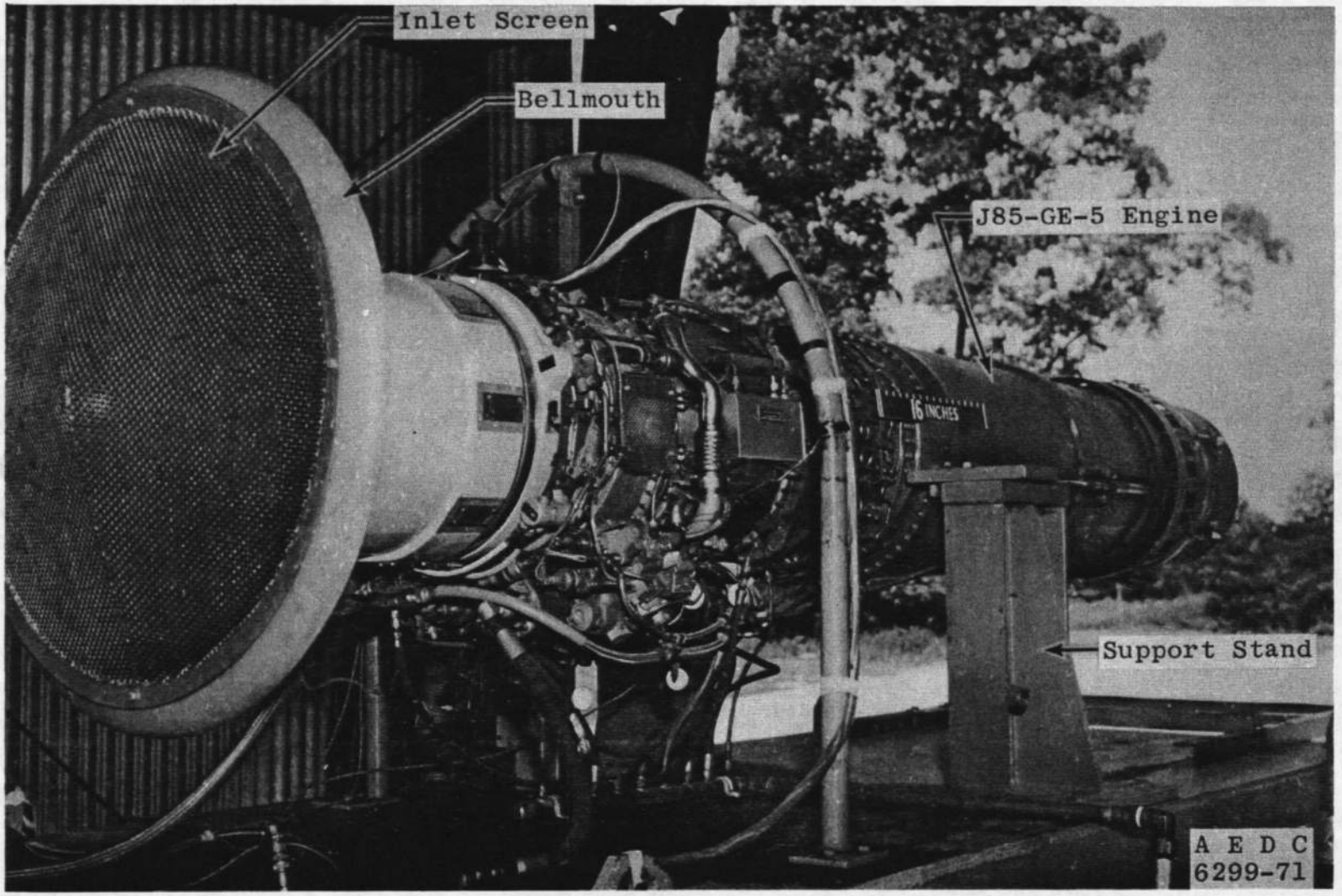

b. As Installed in the Ground Level Test Stand
Fig. 5 Concluded

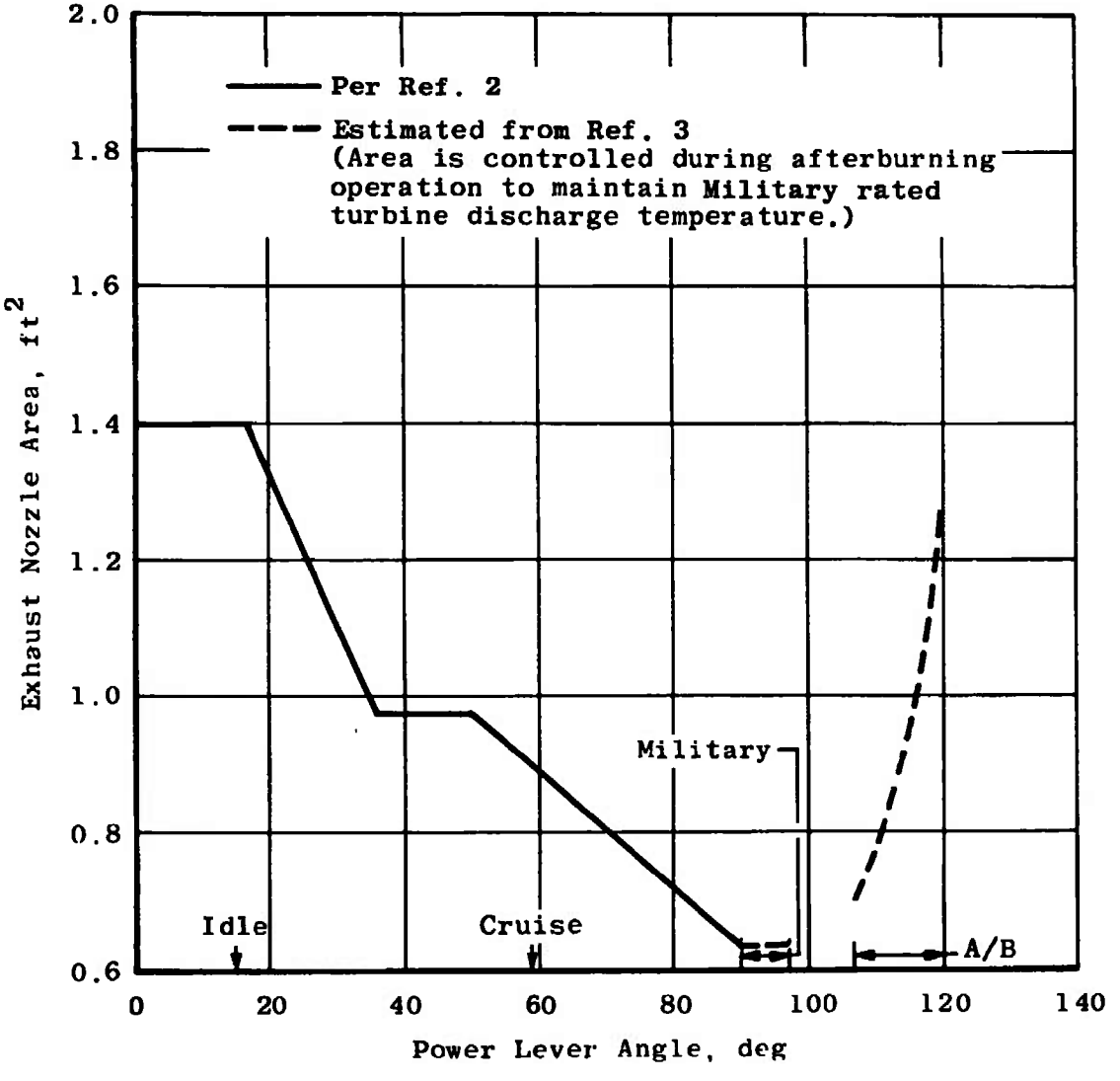

Fig. 6 Exhaust Nozzle Area Schedule

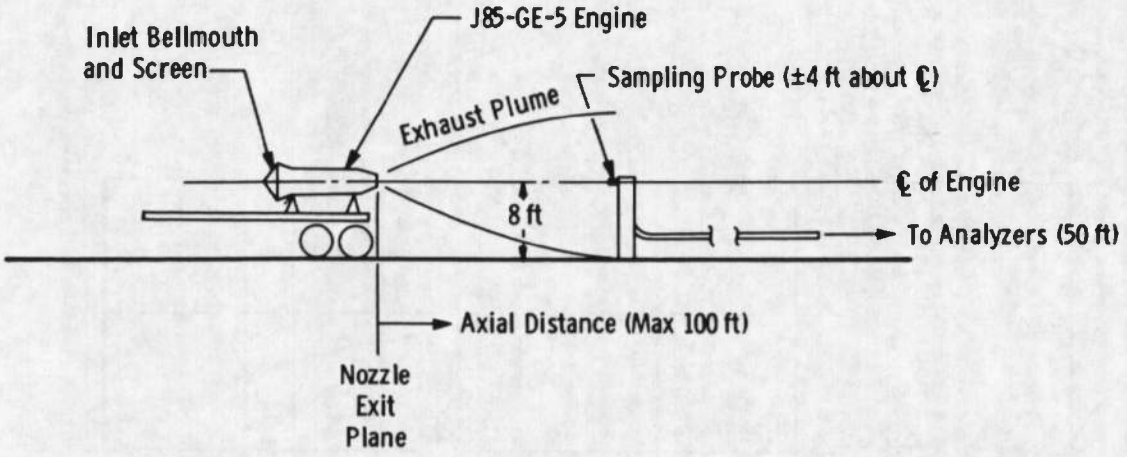

a. Schematic

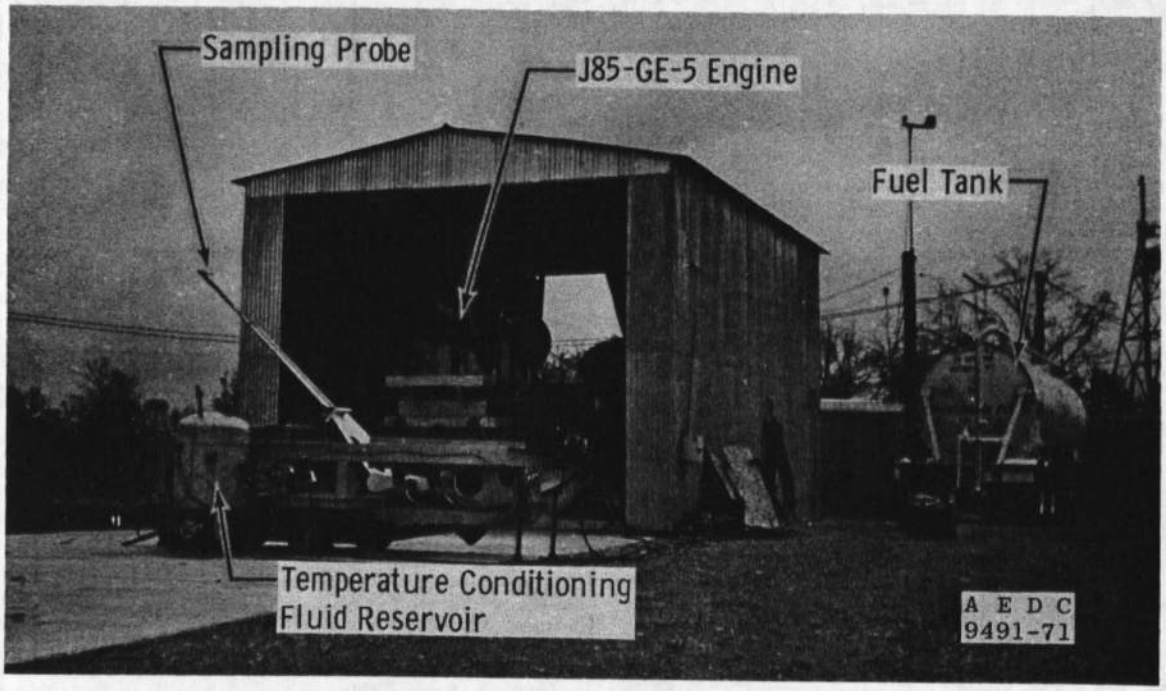

b. Photograph

Fig. 7 Ground Level Test Stand Showing the J85-GE-5 Engine and Emissions Sampling Probe

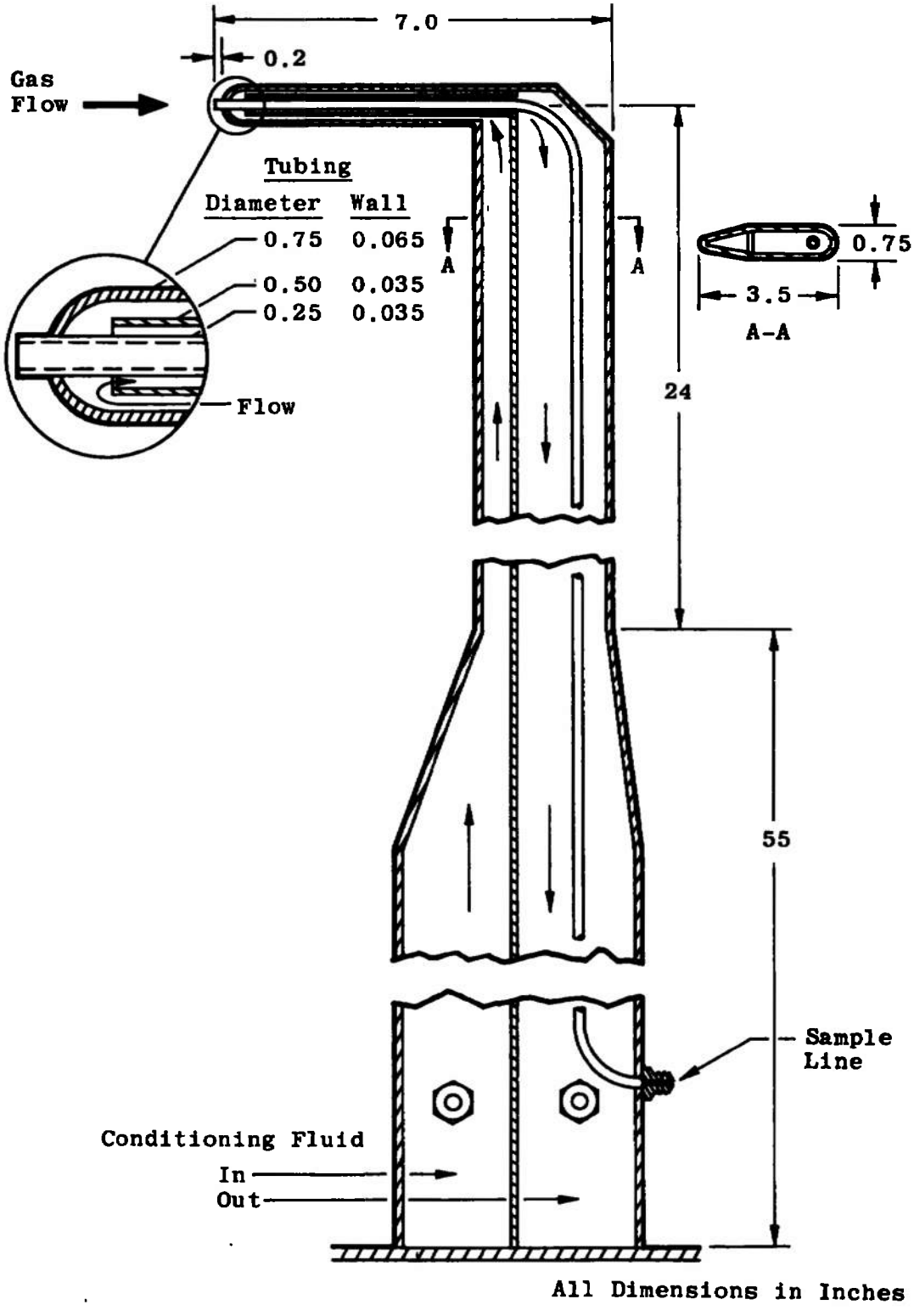

c. Sampling Probe Details
Fig. 7 Concluded

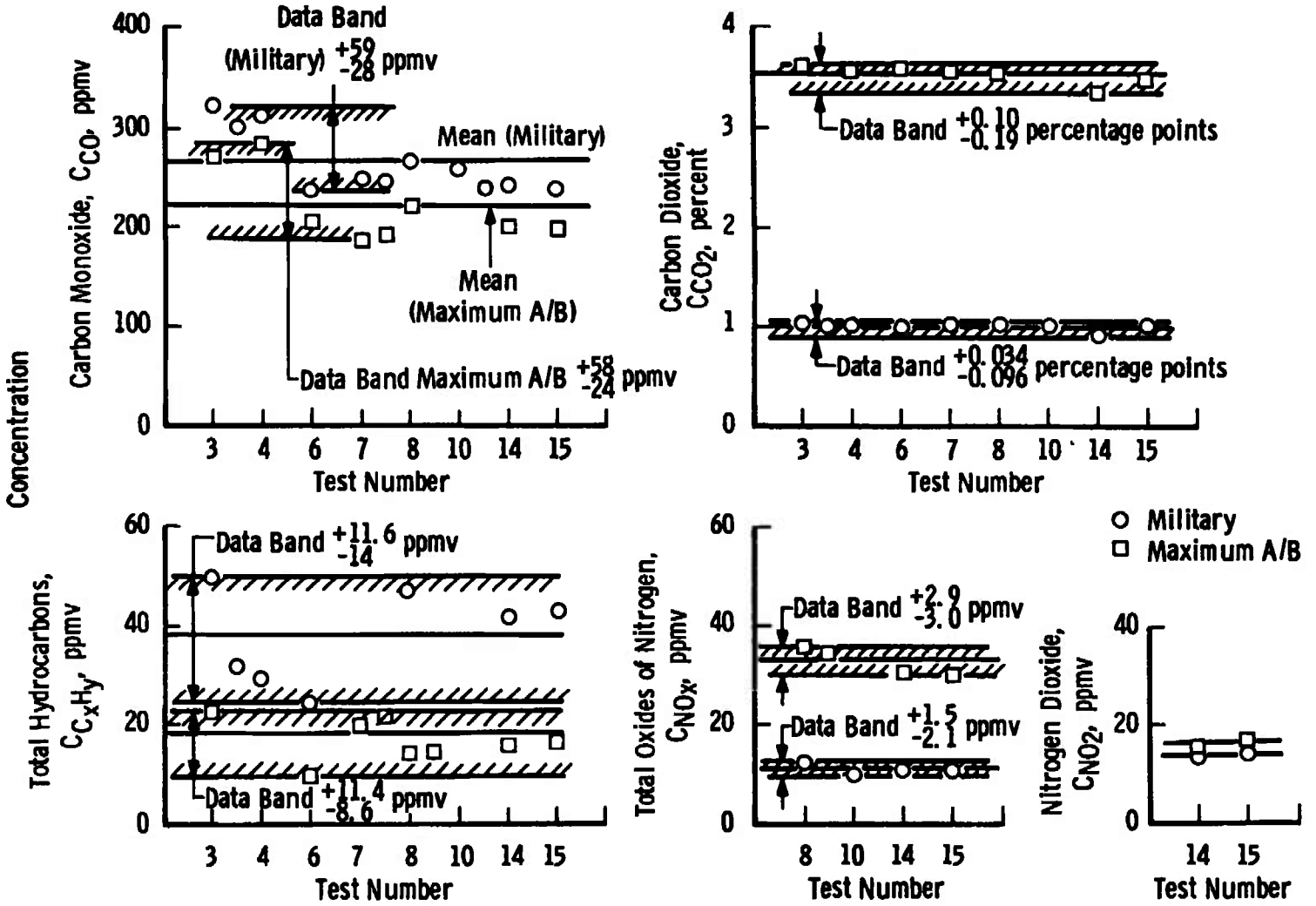

Fig. 8 Variation in Centerline Concentrations of Gaseous Emissions at 16 ft Aft for Military and Maximum Afterburning Power Levels as a Function of Test Number

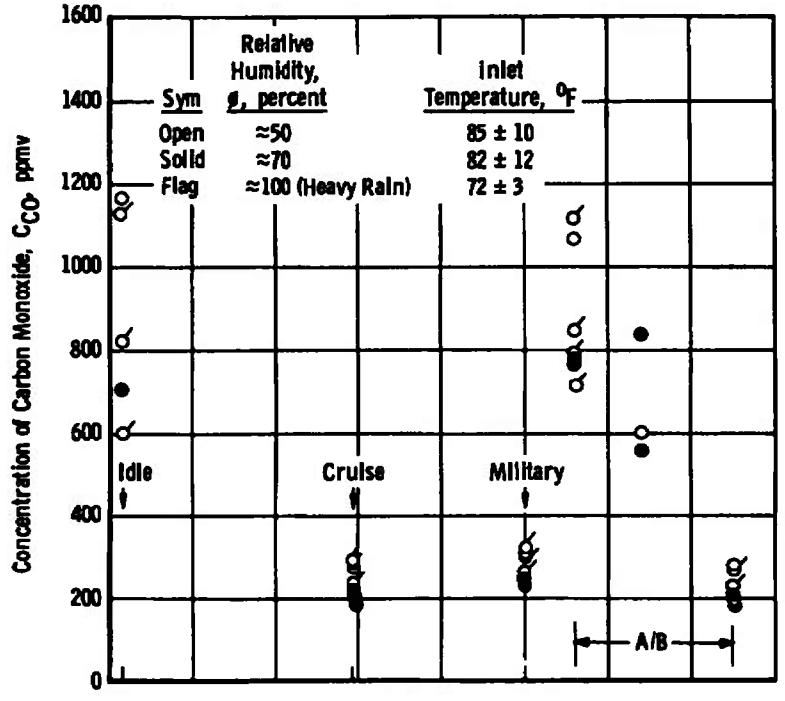

a. Carbon Monoxide

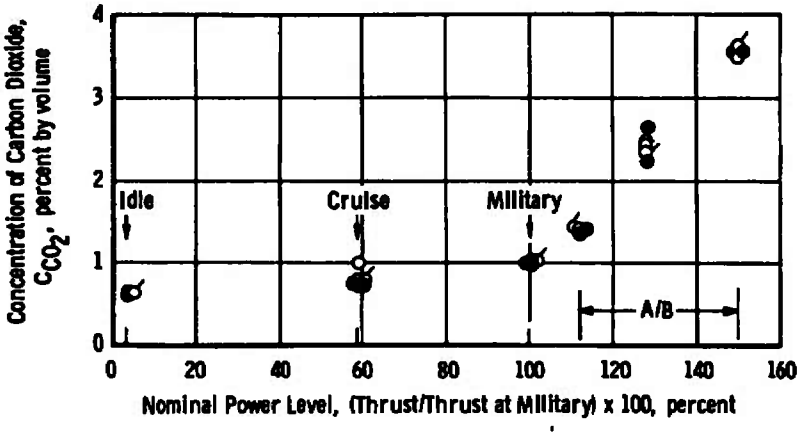

b. Carbon Dioxide

Fig. 9 Effects of Relative Humidity and Rain on Centerline Pollutant Concentrations at 16 ft Aft of the Engine

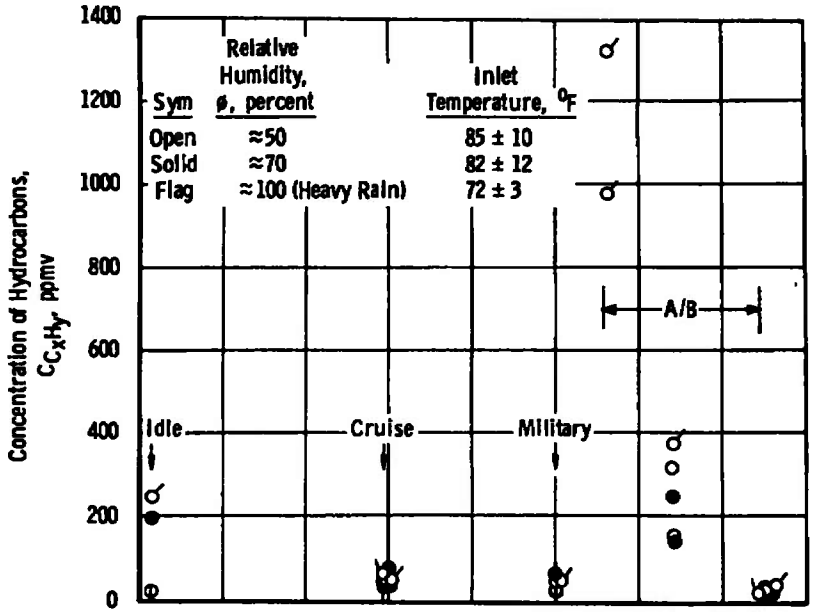

c. Hydrocarbons

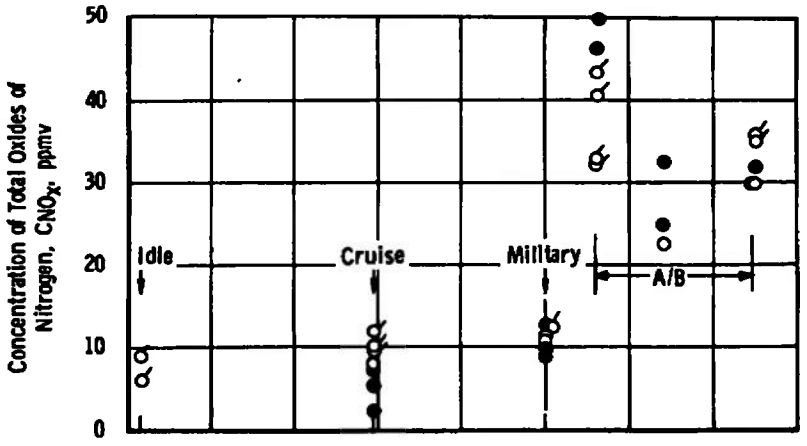

d. Total Oxides of Nitrogen

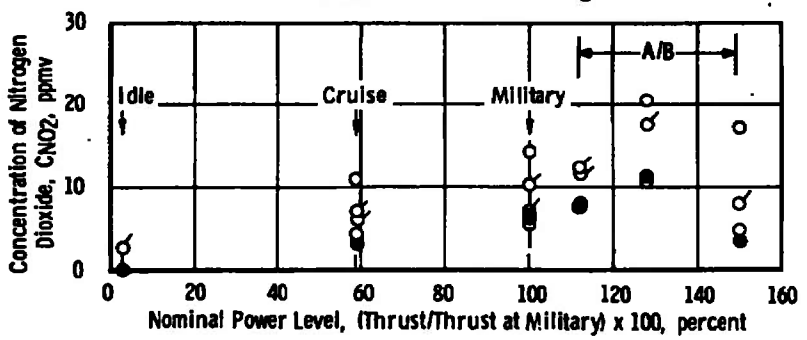

e. Nitrogen Dioxide

Fig. 9 Concluded

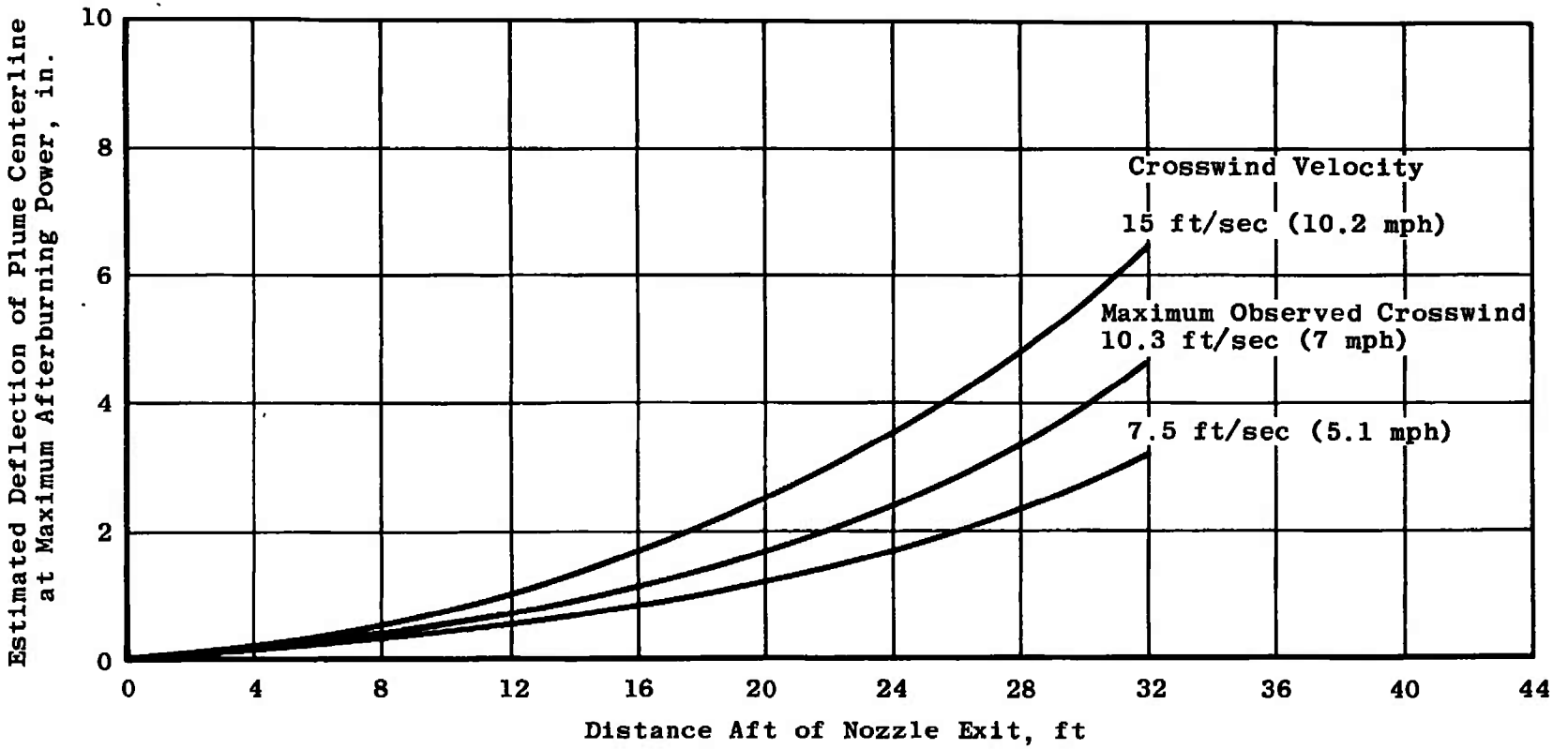

Fig. 10 Estimated Crosswind Deflection of Plume Centerline at Maximum Afterburning

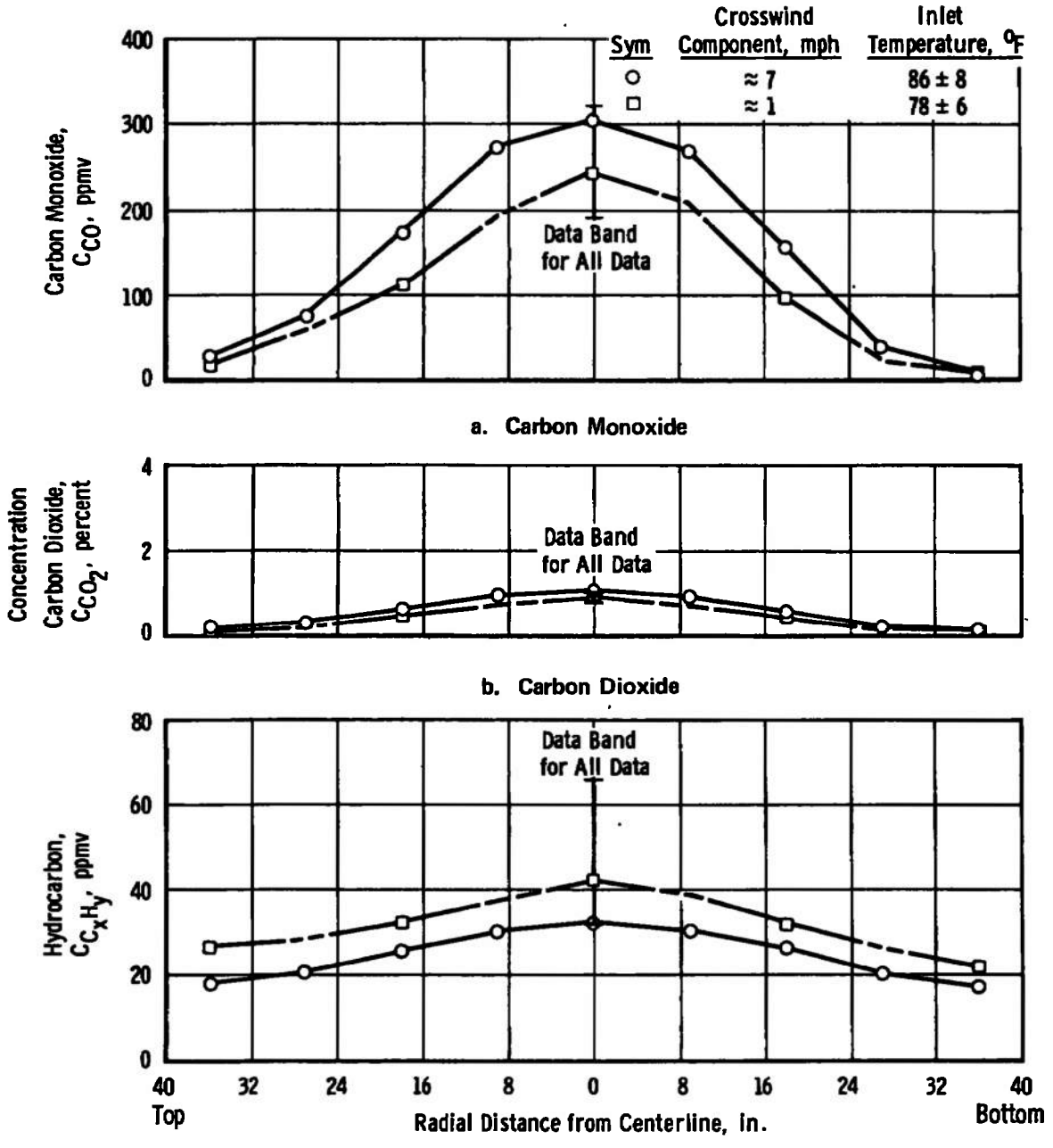

Fig. 11 Effects of Crosswind on Radial Distribution of Pollutants at Military Power, 16 ft Aft of the Nozzle Exit Plane

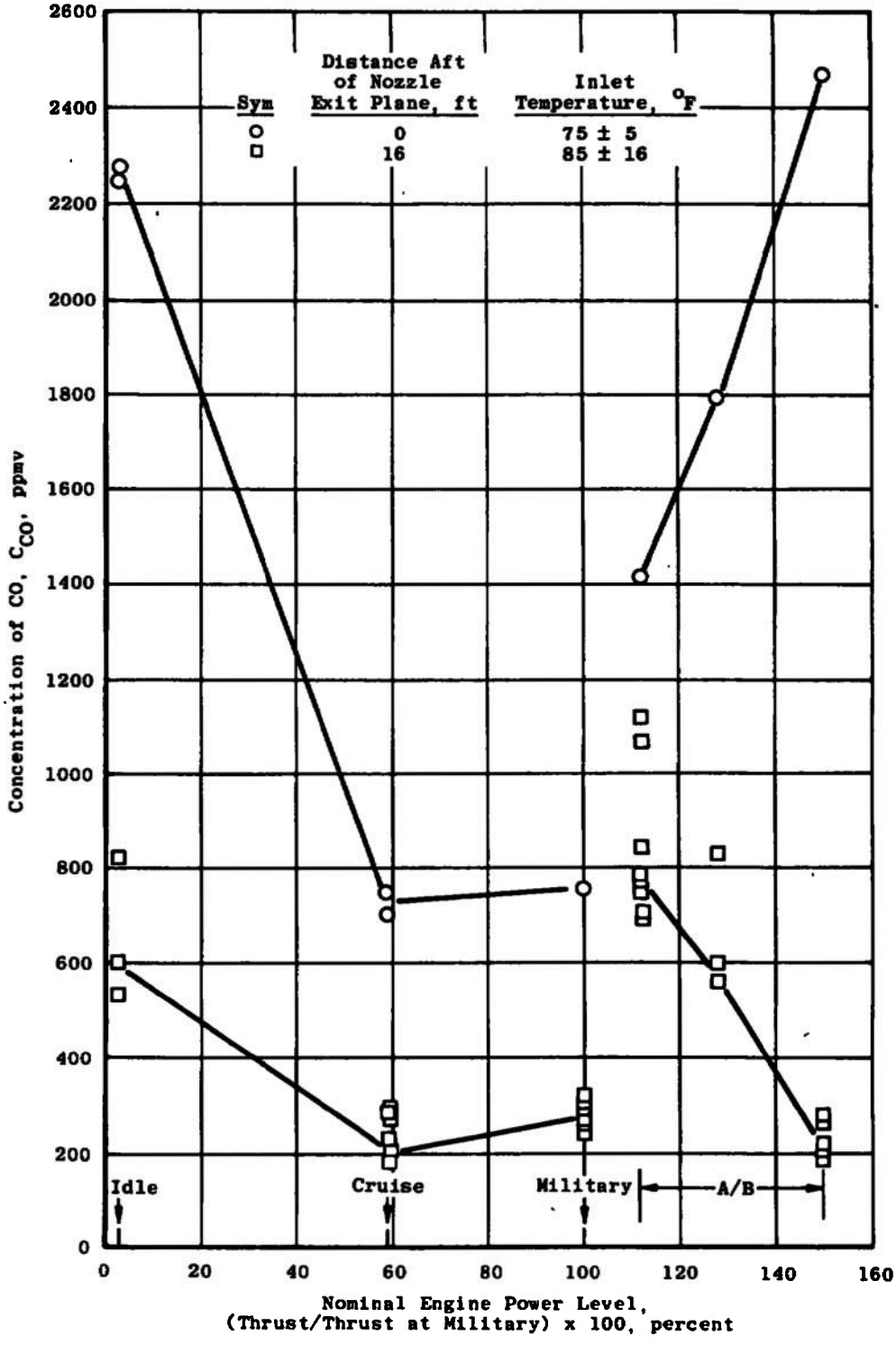

a. Carbon Monoxide

Fig. 12 Pollutant Concentration as a Function of Engine Power Level at the Nozzle Exit and 16 ft Aft of the Nozzle Exit Plane

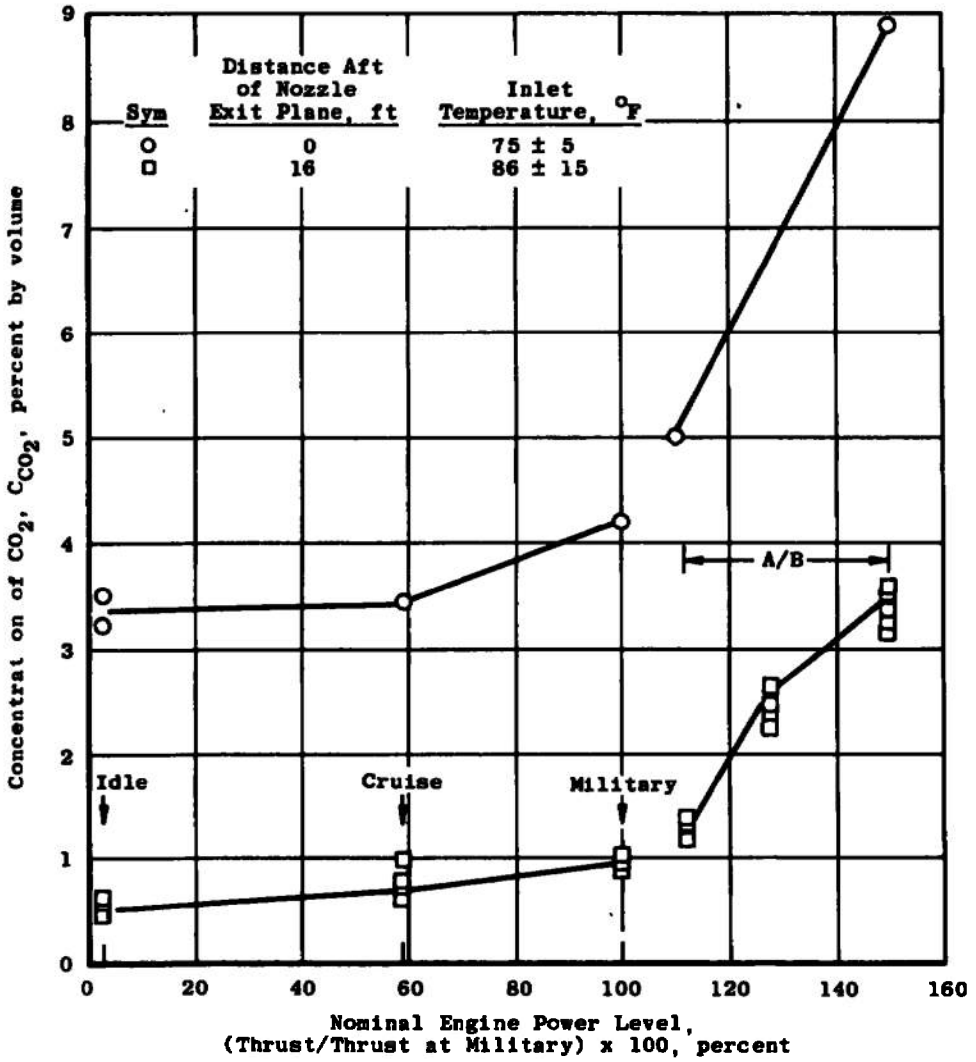

b. Carbon Dioxide
Fig. 12 Continued

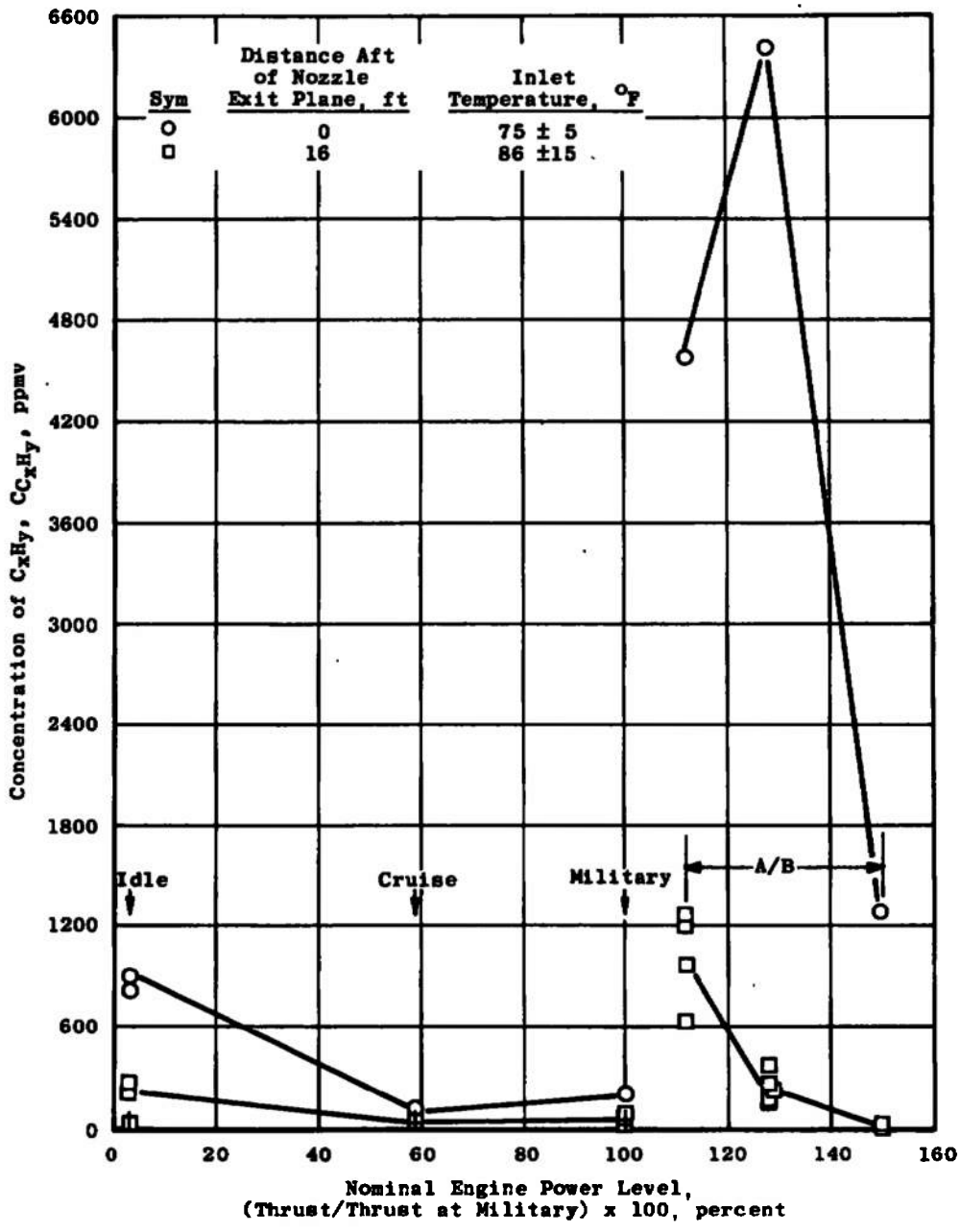

c. Hydrocarbons

Fig. 12 Continued

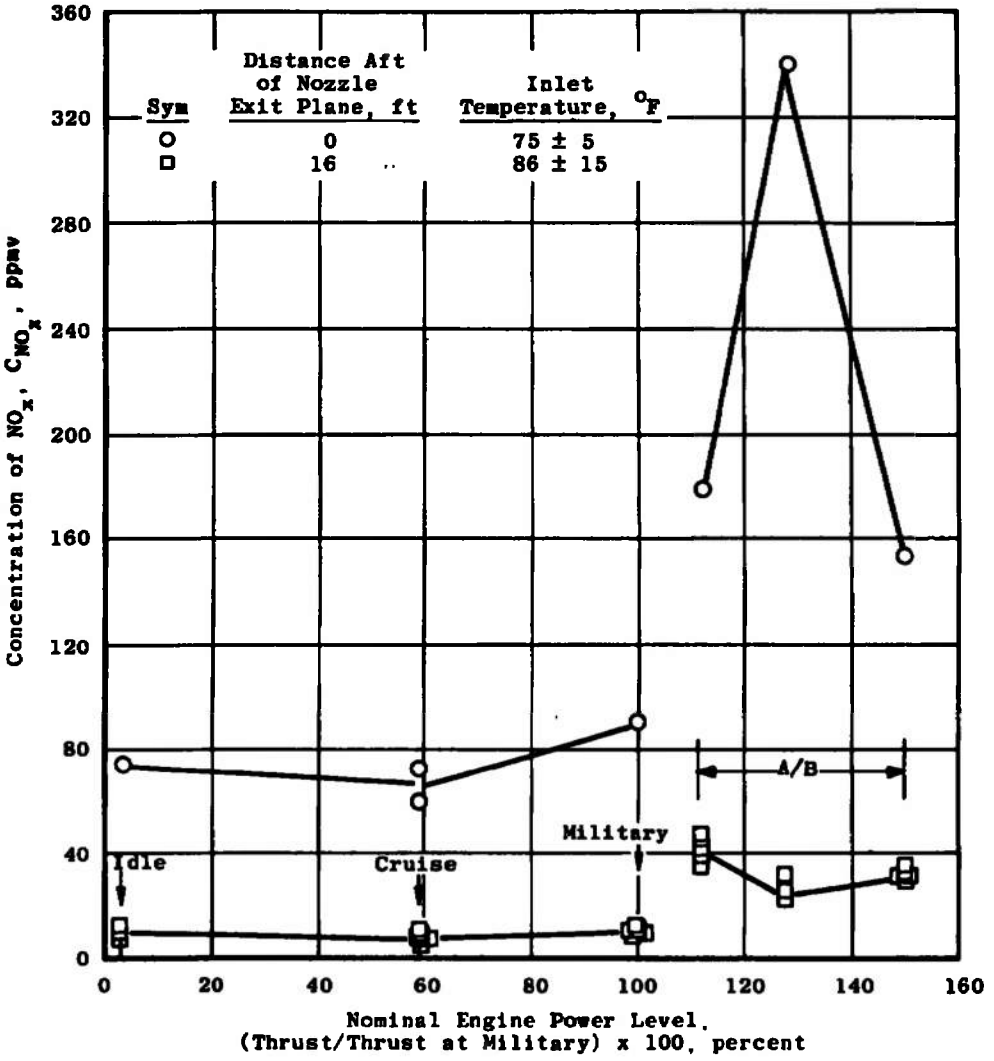

d. Oxides of Nitrogen
Fig. 12 Continued

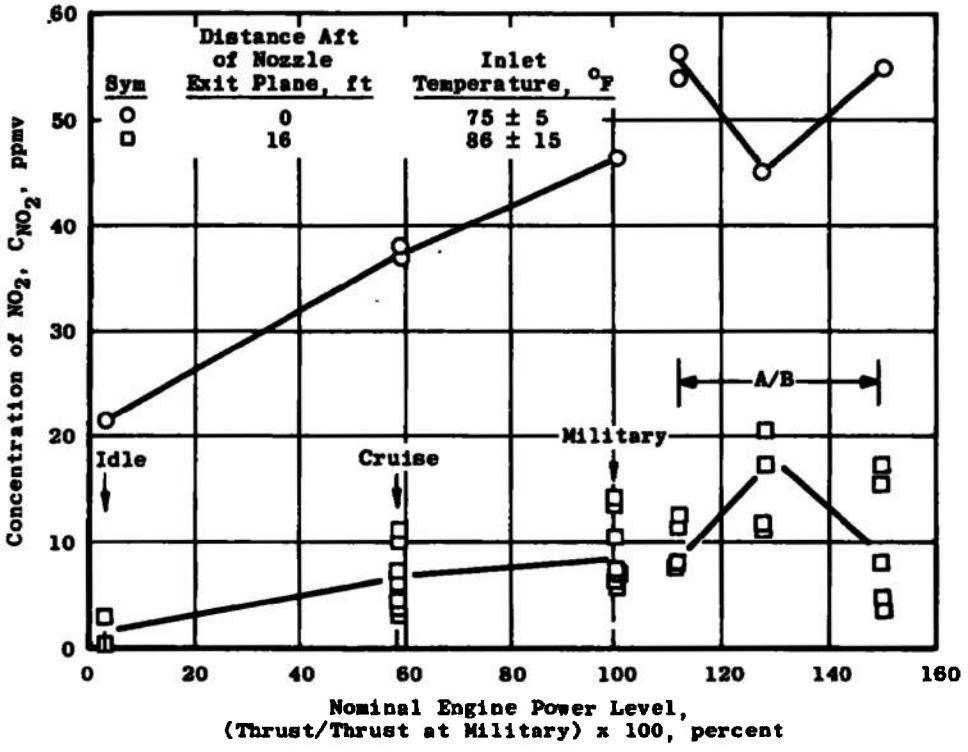

e. Nitrogen Dioxide

Fig. 12 Concluded

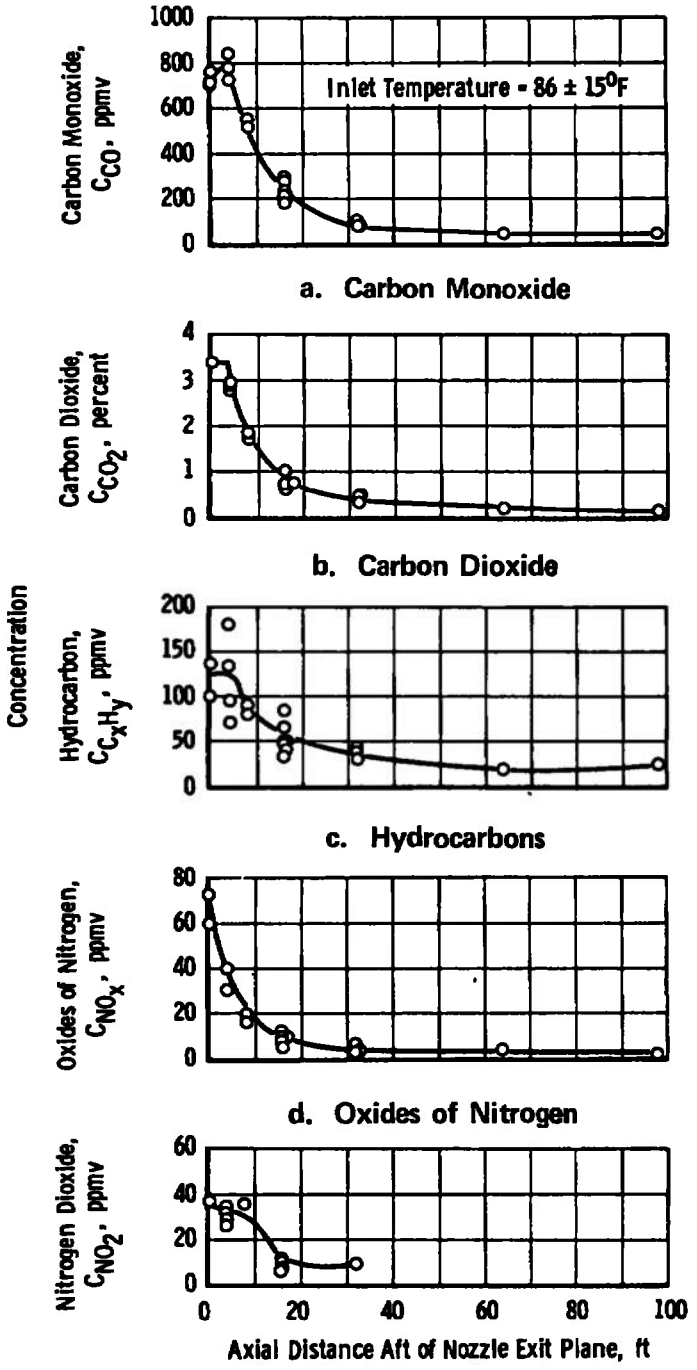

Fig. 13 Centerline Pollutant Concentration as a Function of Axial Distance from the Nozzle Exit Plane at Cruise Power

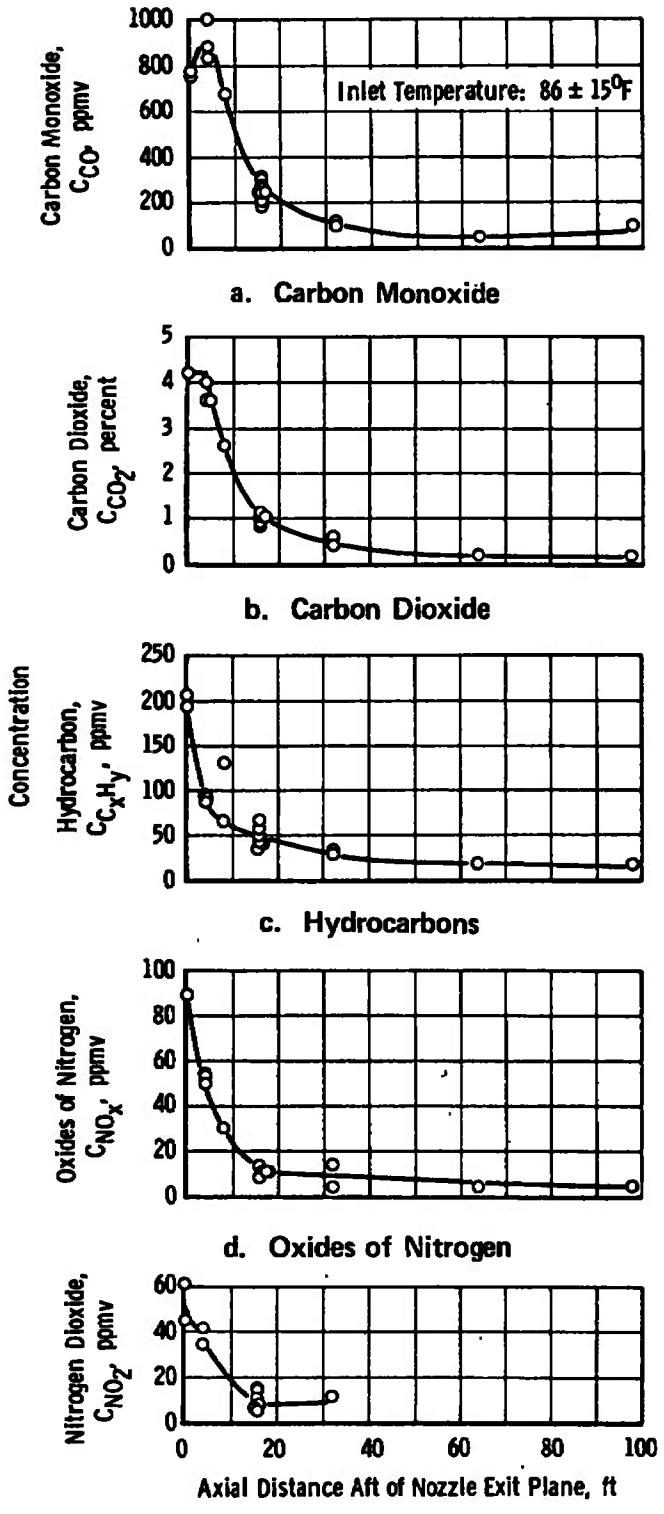

Fig. 14 Centerline Pollutant Concentration as a Function of Axial Distance from the Nozzle Exit Plane at Military Power

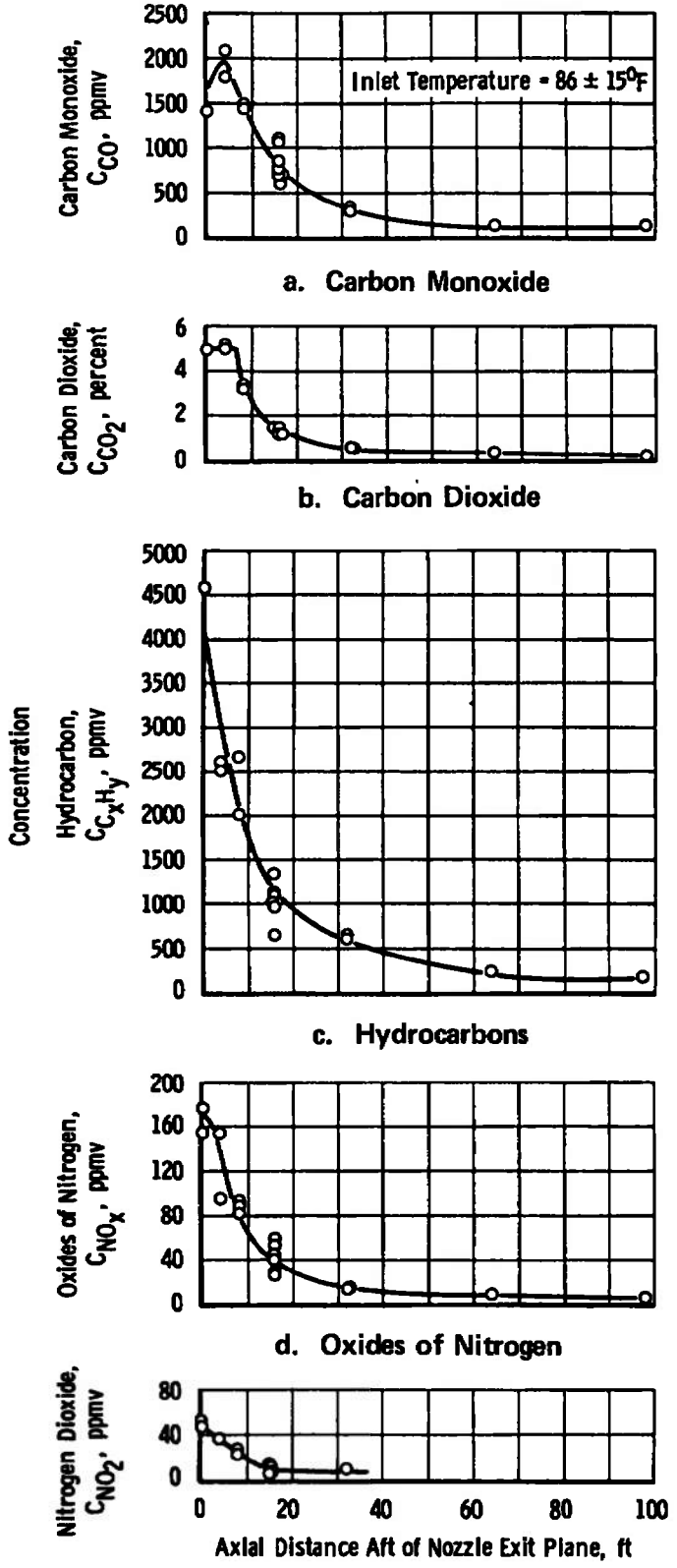

Fig. 15 Centerline Pollutant Concentration as a Function of Axial Distance from the Nozzle Exit Plane at Minimum A/B Power

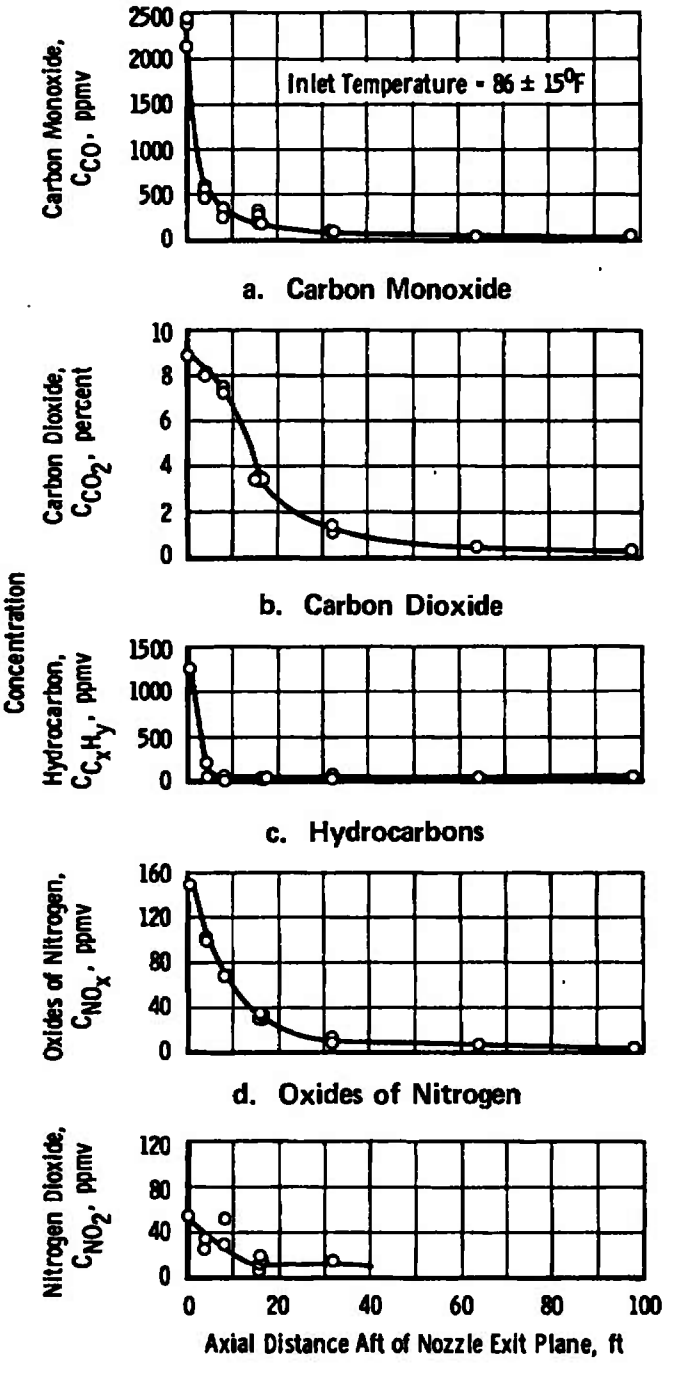

Fig. 16 Centerline Pollutant Concentration as a Function of Axial Distance from the Nozzle Exit Plane at Maximum A/B Power

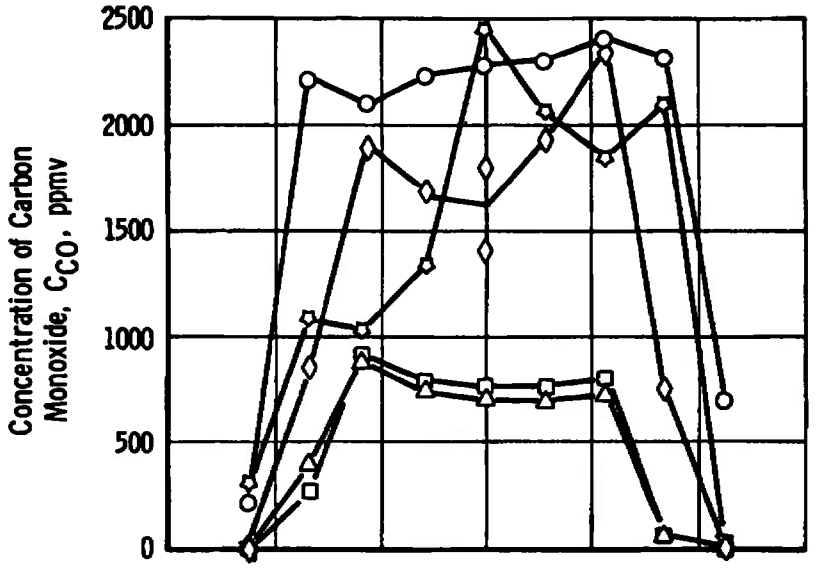

a. Carbon Monoxide

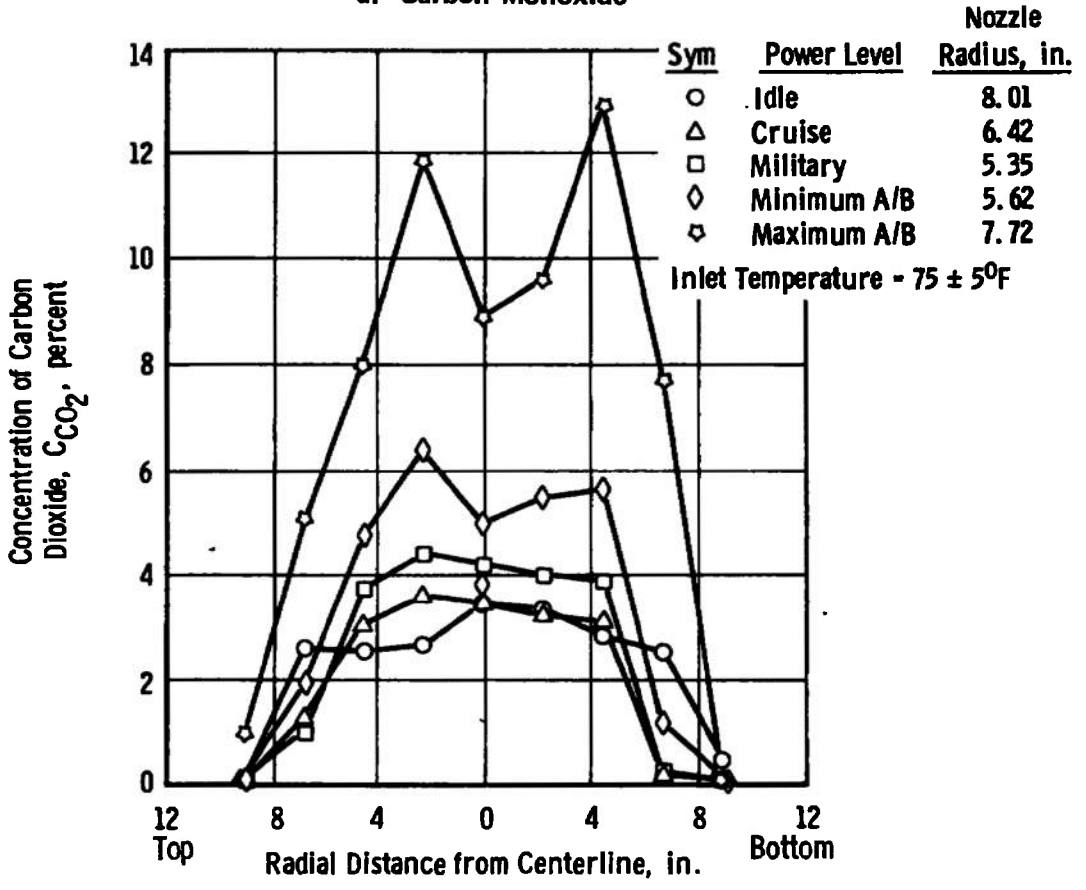

b. Carbon Dioxide

Fig. 17 Effects of Power Level on the Radial Distribution of Pollutant Concentration at the Nozzle Exit

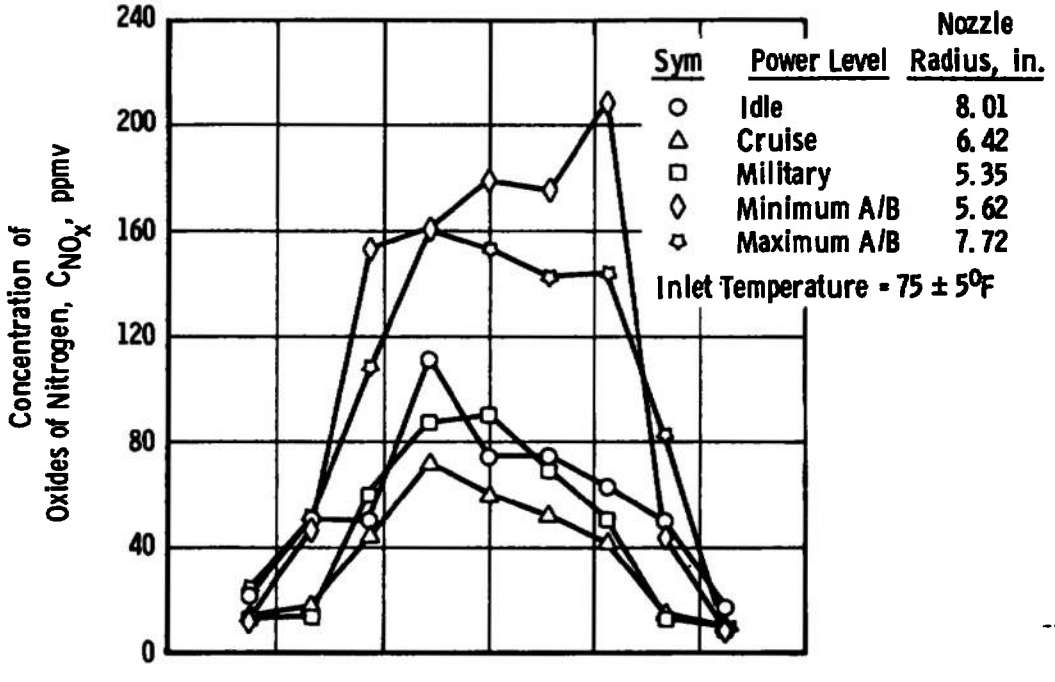

d. Oxides of Nitrogen

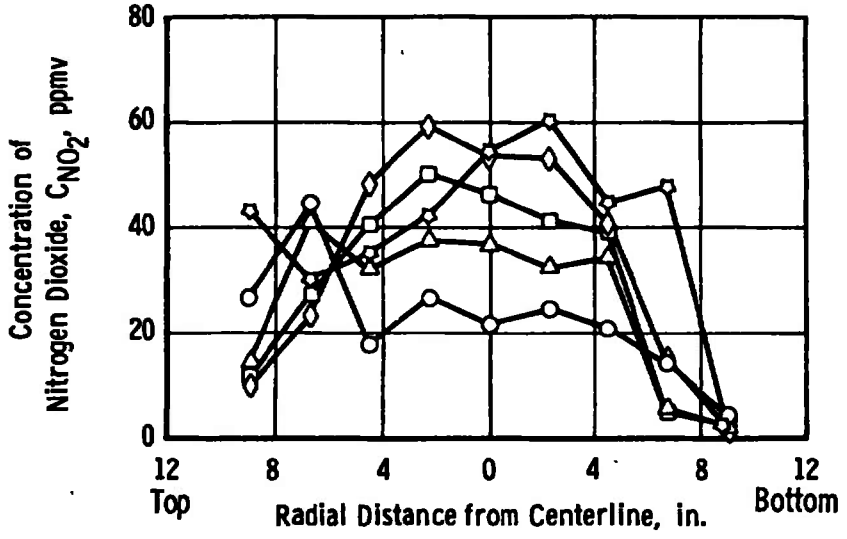

e. Nitrogen Dioxide

Fig. 17 Concluded

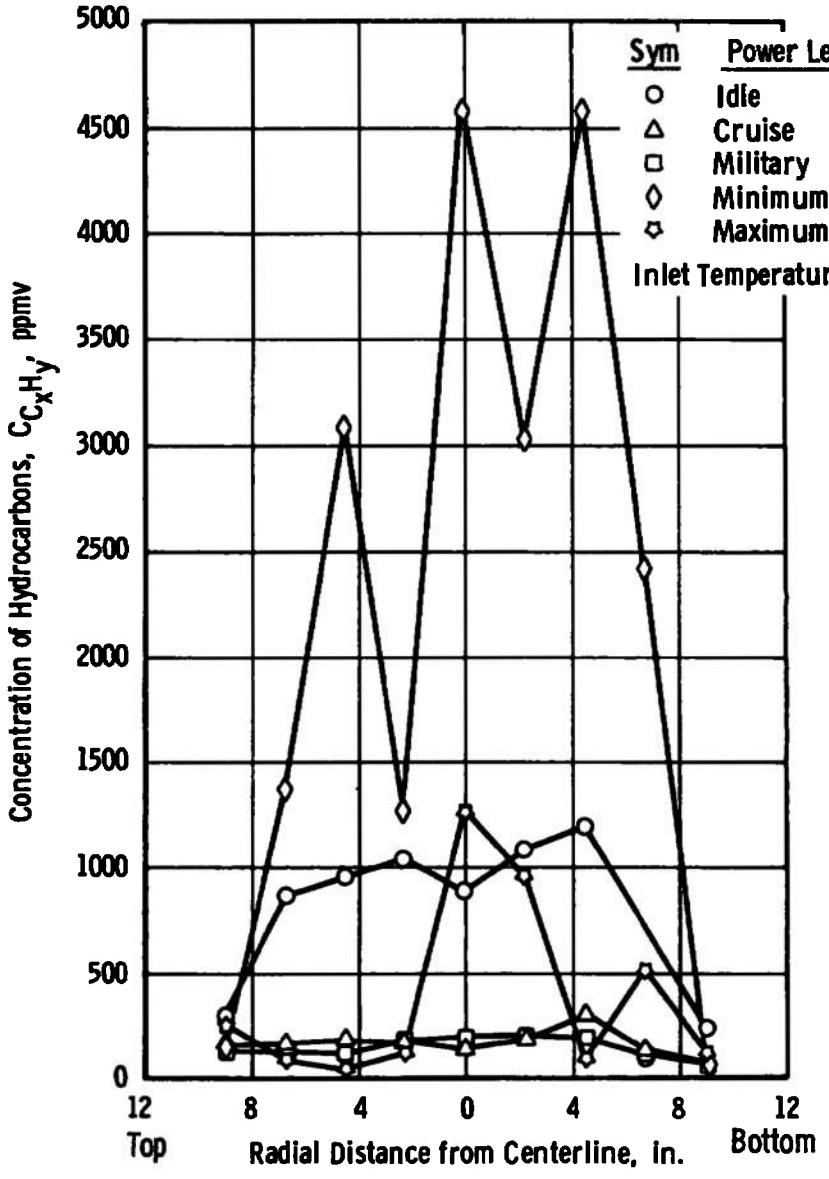

c. Hydrocarbons

Fig. 17 Continued

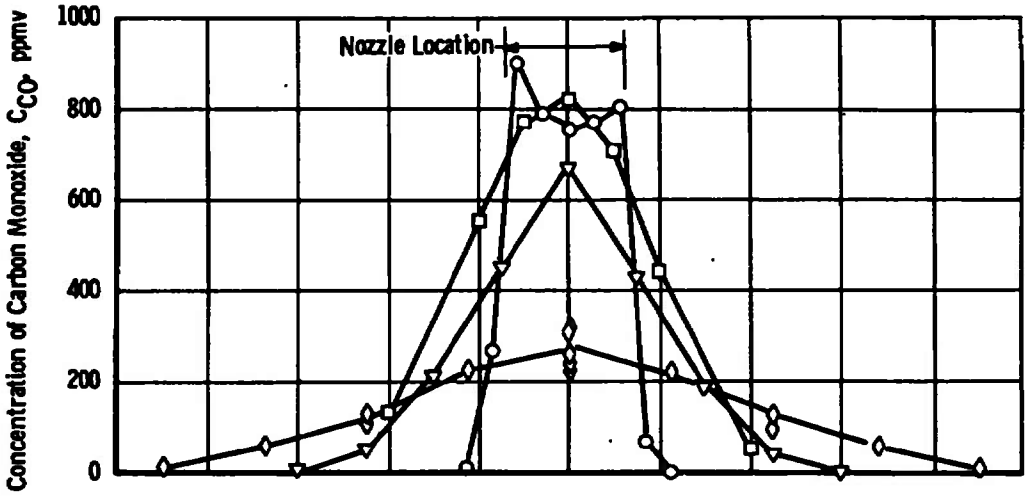

a. Carbon Monoxide

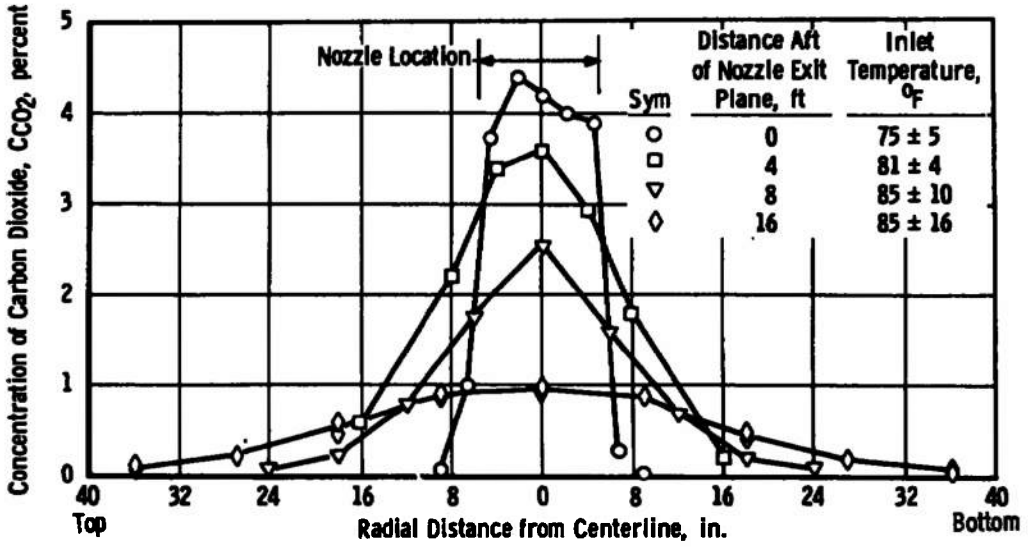

b. Carbon Dioxide

Fig. 18 Effects of Axial Distance on the Radial Distribution of Pollutant Concentrations at Military Power

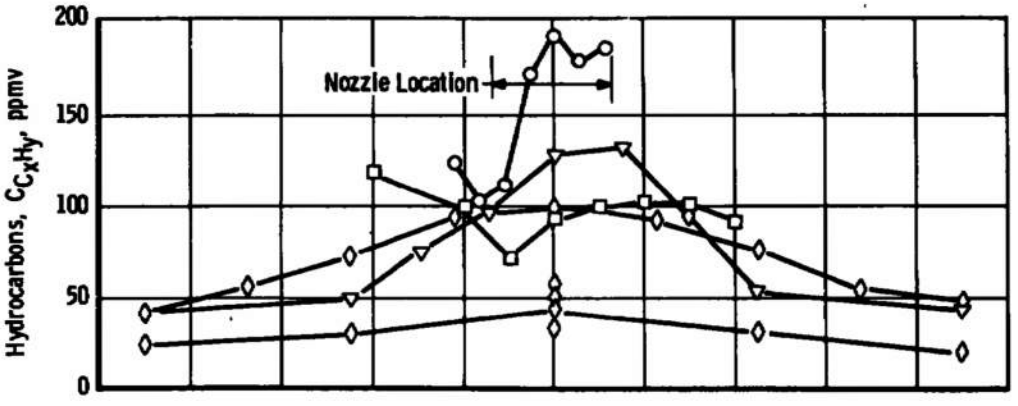

c. Hydrocarbons

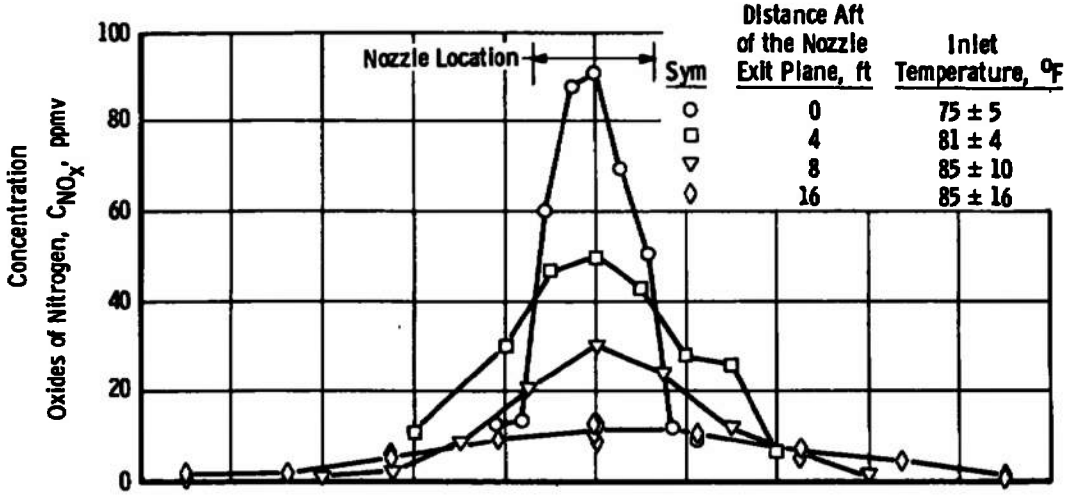

d. Oxides of Nitrogen

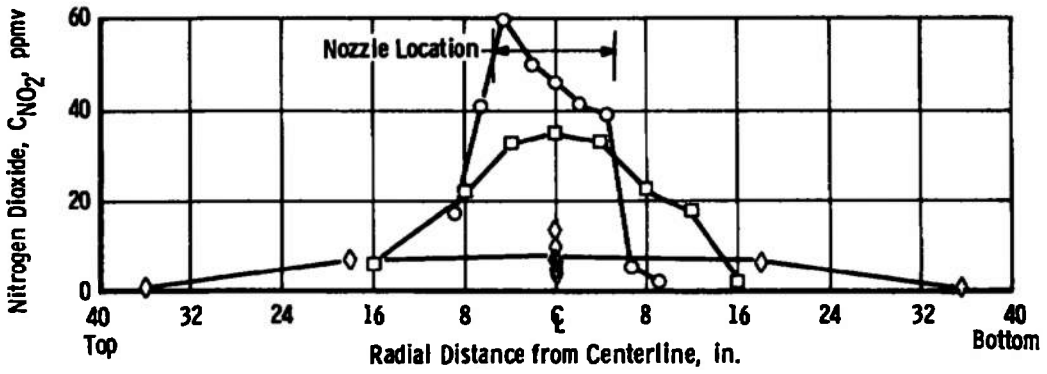

e. Nitrogen Dioxide

Fig. 18 Concluded

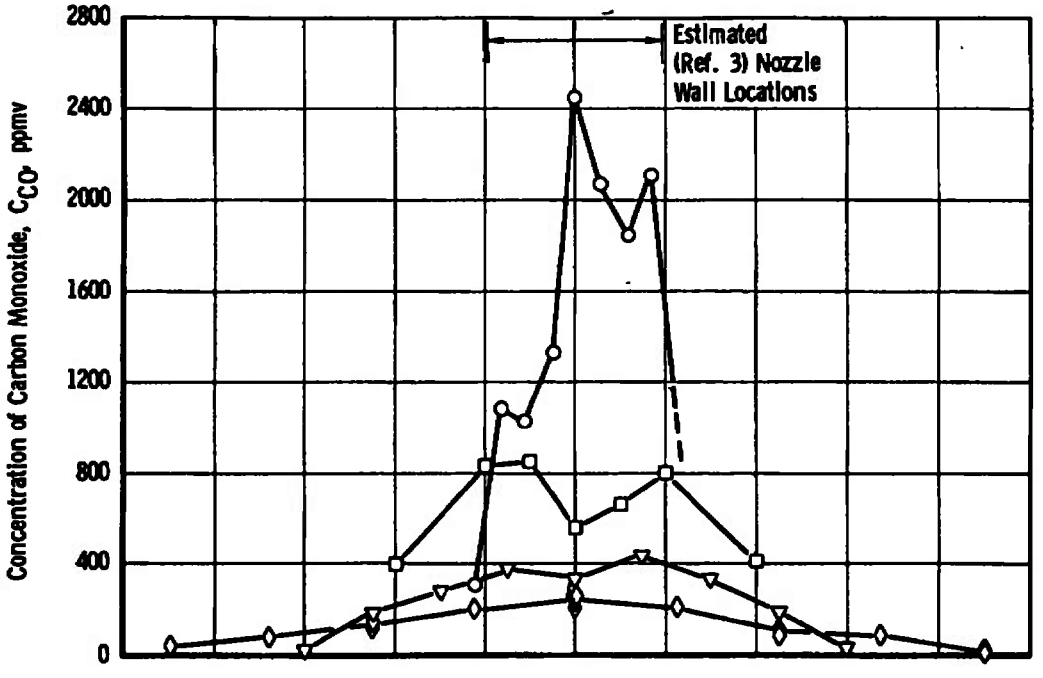

a. Carbon Monoxide

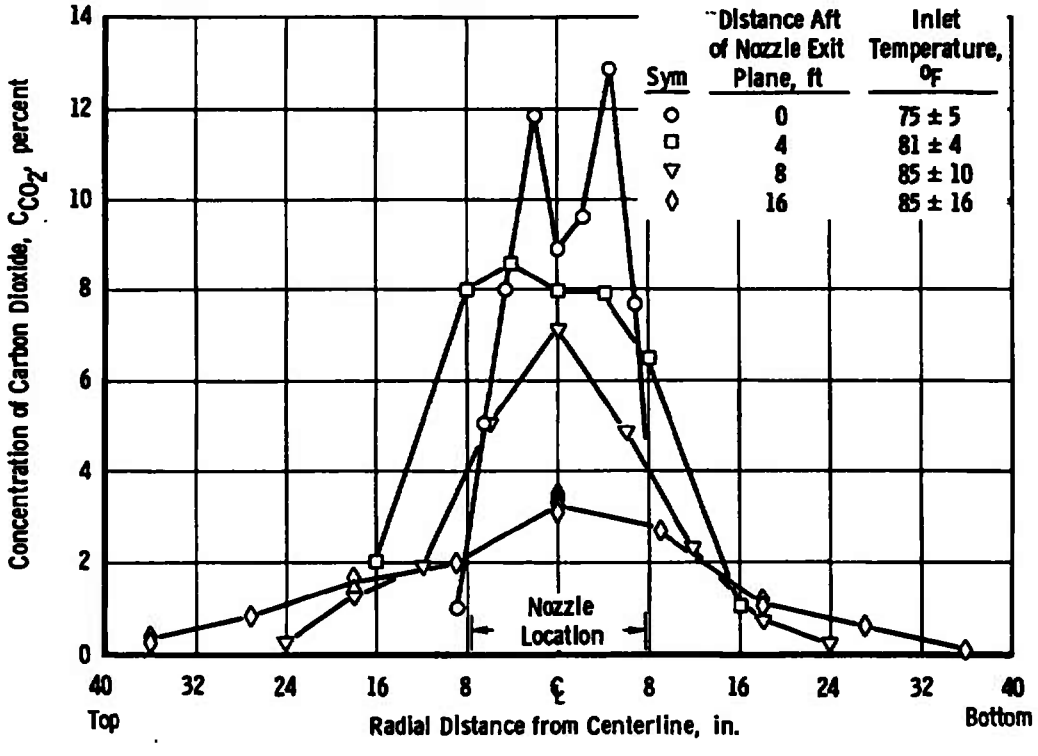

b. Carbon Dioxide

Fig. 19 Effects of Axial Distance on the Radial Distribution of Pollutant Concentrations at Maximum A/B Power

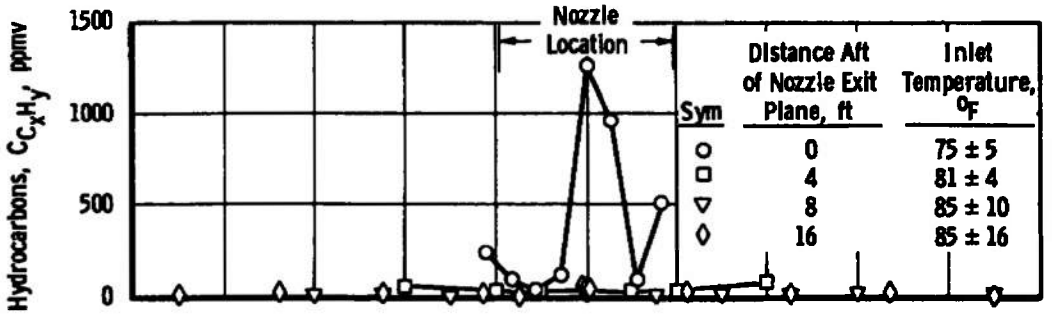

c. Hydrocarbons

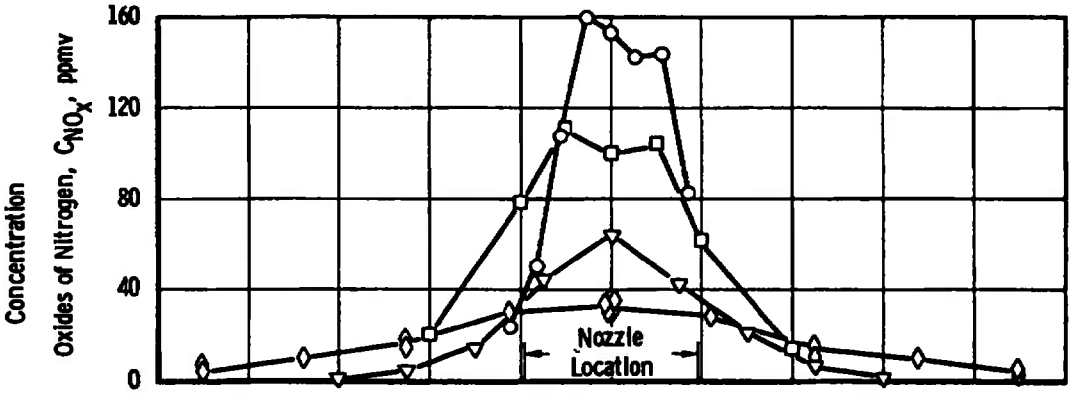

d. Oxides of Nitrogen

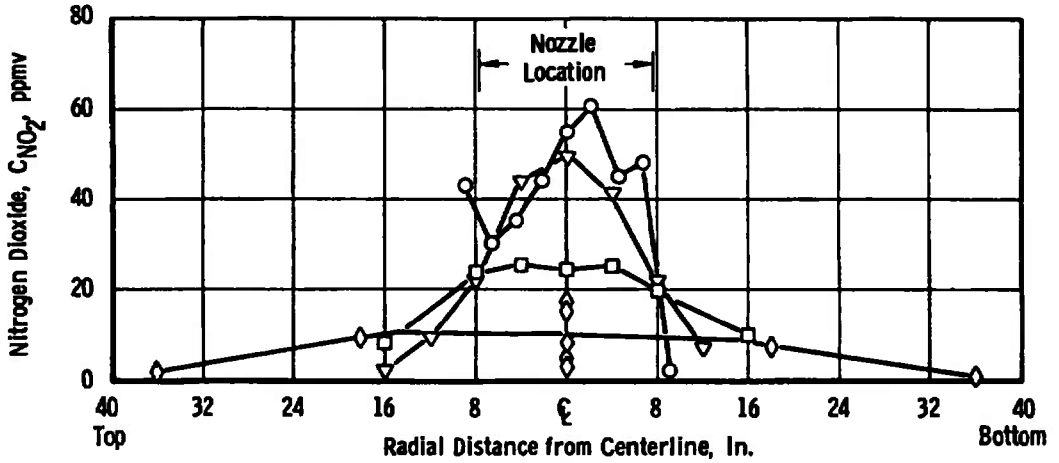

e. Nitrogen Dioxide

Fig. 19 Concluded

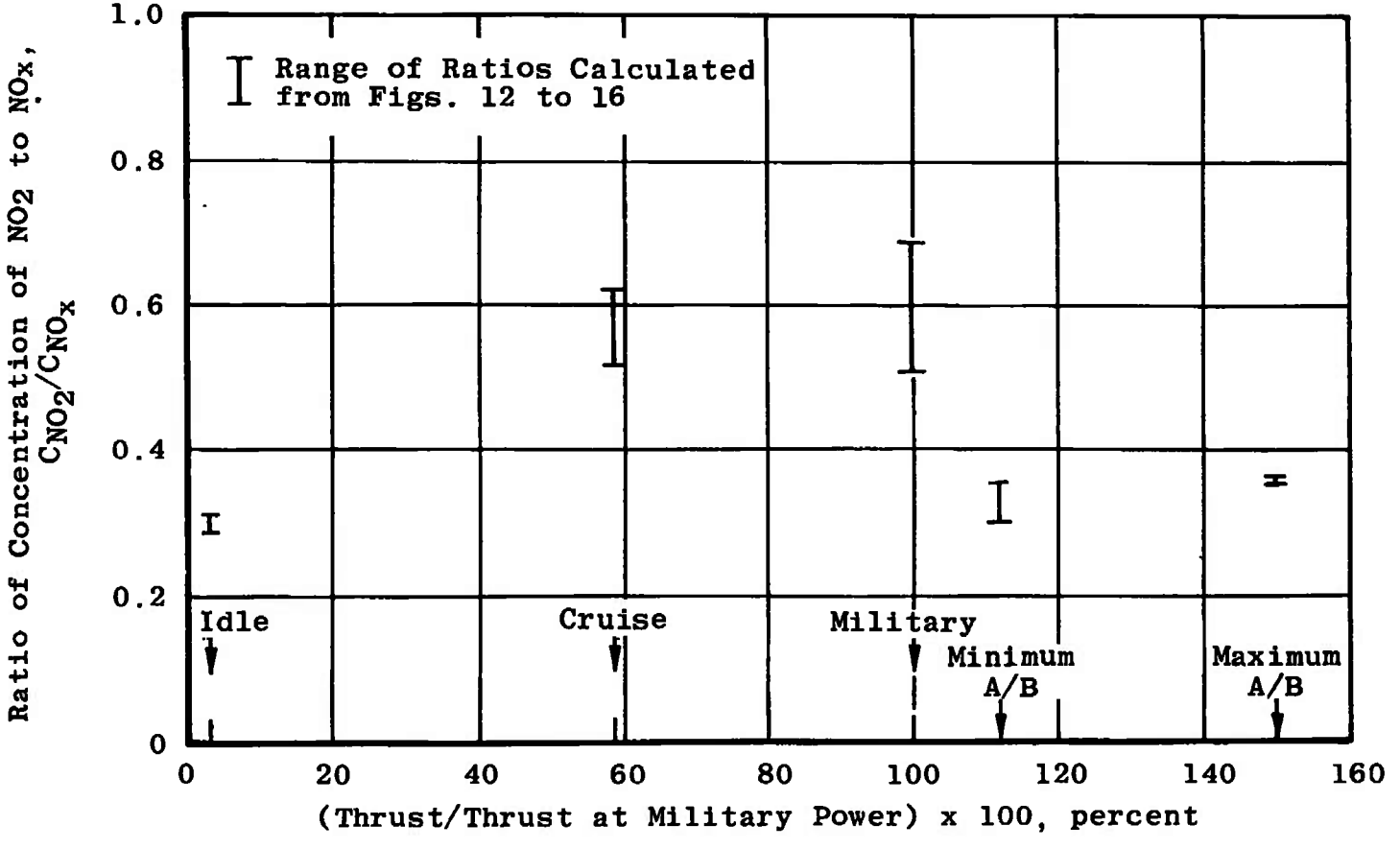

Fig. 20 Ratio of Centerline Concentration of Nitrogen Dioxide to Total Oxides of Nitrogen Concentration as a Function of Engine Power Level

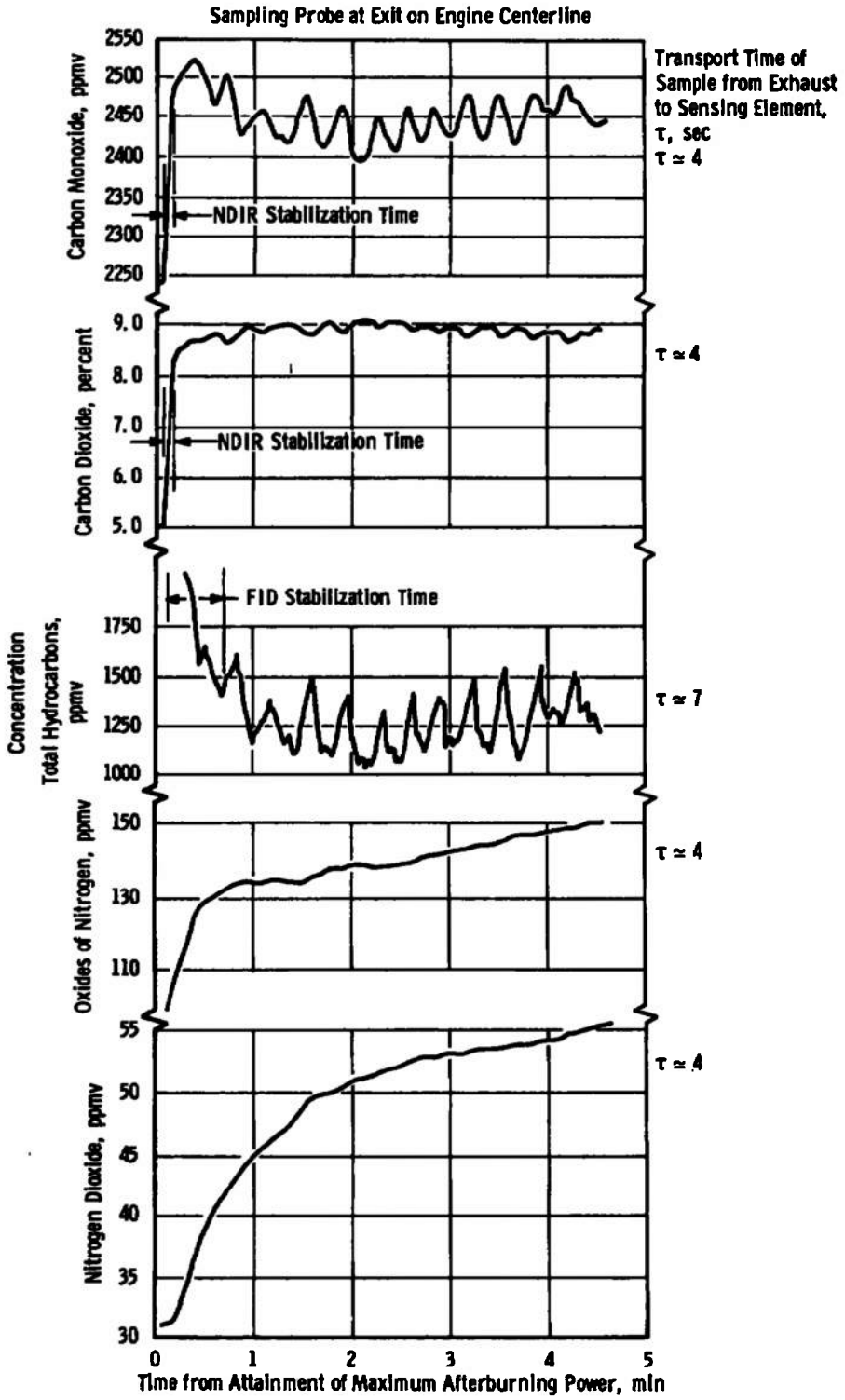

Fig. 21 Cyclical Combustion Variation at Maximum Afterburning Power Level

TABLE I
J85-GE-5 ESTIMATED PERFORMANCE PARAMETERS WITH 14.2-PSIA INLET PRESSURE AND 59-DEG F INLET TEMPERATURE FOR THE POWER LEVELS USED FOR POLLUTION MEASUREMENTS[1]

Nominal Power Level	Engine Airflow, lbm/sec	$\frac{\text{Thrust}}{\text{Thrust at Military}} \times 100$	Engine Speed, N, percent Rated	Fuel Flow, lbm/hr		Exhaust Gas Temperature, EGT, °R	Calculated Turbine Inlet Temperature, °R (Ref. 3)	Time Limit of Power
				Engine	A/B			
Idle	12.5	3.0 percent	50.0	650	---	1460	---	Continuous
Cruise[2]	37.6	59.0 percent	95.0	1800	---	1610	1785	Continuous[2]
Military	42.5	100.0 percent[5]	100.0	2650	---	1710	2150	30 min
Minimum A/B	42.5	112.0 percent	~100.0	2650	1000	---	2150	---[3]
Middle A/B	42.5	128.0 percent	~100.0	2650	2950	---	2145	---[3]
Maximum A/B	42.5	150.0 percent	~100.0	2650	4050	~3300[4]	2140	5 min

[1]See Refs. 3 and 4

[2]Maximum Power for Continuous Operation

[3]Not Specified

[4]Nozzle Discharge Temperature

[5]Thrust at Military Power with Inlet Temperature of 519°R is Approximately 2450 lbf

TABLE II
CHEMICAL COMPOSITION OF JP-4 FUEL[1]

Constituent	Maximum Allowable
Sulfur	0.4 percent weight
Mercaptan Sulfur	0.001 percent weight
Aromatics	25.0 percent volume
Olefin	5.0 percent volume
Particulate Matter	8.0 mg/gal
Fuel System Icing Inhibitor	0.15 percent volume[2]
Anti-Oxidants[3]	9.1 g/100 gal
N, N′ - Diisopropyl-para-phenylenediamine	
N, N′ - Disecondary Butyl-para-phenylenediamine	
2, 6 Ditertiary Butyl-4-methylphenol	
2, 4 Dimethyl-6-Tertiary butylphenol	
2, 6 Ditertiary Butylphenol	
75-percent Minimum 2, 6 - Ditertiary Butylphenol and 25-percent Maximum Tertiary and Tritertiary Butylphenols	

[1]The fuel shall consist completely of hydrocarbon compounds except as specified in MIL-T-5624G.

[2]Minimum of 0.10 percent volume.

[3]Listed items may be blended separately or in combination not in excess of specified limit.

TABLE III
STEADY-STATE MEASUREMENT UNCERTAINTY

Parameter Designation Exhaust Gas Emissions Concentration:	STEADY-STATE ESTIMATED MEASUREMENT*									Type of Measuring Device	Type of Recording Device	Method of System Calibration
	Precision Index (S)			Bias (B)			Uncertainty $\pm(B + t_{95}S)$					
	Percent of Reading	Unit of Measurement	Degree of Freedom	Percent of Reading	Unit of Measurement		Percent of Reading	Unit of Measurement	Range			
Carbon Monoxide, CO, ppmv	---	±1.65 ppmv	30	---	± 8.7 ppmv		---	± 12 ppmv	0 to 300 ppmv	Continuous Process Nondispersive Infrared Detector	Null-Balance Potentiometer Strip-Chart Recorder	In-Place Application of Gas of Concentration Determined in the Standards Laboratory
		±2.75 ppmv			±14.5 ppmv			± 20 ppmv	0 to 500 ppmv			
		±5.5 ppmv			±29.0 ppmv			± 40 ppmv	0 to 1000 ppmv			
		±16.5 ppmv			±87.0 ppmv			±120 ppmv	0 to 3000 ppmv			
Carbon Dioxide, CO_2, percent	---	±0.022 percent	30	---	±0.116 percent		---	±0.16 percent	0 to 4 percent			
		±0.055 percent			±0.29 percent			±0.40 percent	0 to 10 percent			
		±0.11 percent			±0.58 percent			±0.80 percent	0 to 20 percent			
Total Hydrocarbons, C_xH_y, ppmv	---	±0.43 ppmv	30	---	±2.9 ppmv		---	±3.8 ppmv	0 to 100 ppmv	Continuous Process Flame Ionization Detector		
		±4.3 ppmv			±29.0 ppmv			±38 ppmv	0 to 1000 ppmv			
		±8.6 ppmv			±58.0 ppmv			±75 ppmv	0 to 2000 ppmv			
		±34.4 ppmv			±232 ppmv			±301 ppmv	0 to 8000 ppmv			
Total Oxides of Nitrogen, NO_x, ppmv	---	±0.35 ppmv	30	---	±2.85 ppmv		---	±3.6 ppmv	0 to 100 ppmv	Continuous Process Electrochemical Device		
		±1.05 ppmv			±8.55 ppmv			±10.7 ppmv	0 to 300 ppmv			
Nitrogen Dioxide, NO_2, ppmv	---	±0.175 ppmv	30	---	±2.7 ppmv		---	±3.05 ppmv	0 to 50 ppmv			
		±0.35 ppmv			±5.4 ppmv			±6.1 ppmv	0 to 100 ppmv			

*Reference: CPIA No. 180, "ICRPG Handbook for Estimating the Uncertainty in Measurements made with Liquid Propellant Rocket Engine Systems," April 30, 1969.

Note: The estimated measurement uncertainty does not include effects of the sample probes and transfer lines.

TABLE IV
TYPICAL TIME VARIATIONS OF THE INDICATED EMISSIONS CONCENTRATIONS DURING OPERATION AT CRUISE POWER

Species	Variation during a 1-min Time Period	Mean Level
CO	±13 ppmv	740 ppmv
CO_2	±0.015 percentage points	2.60 percent
C_xH_y	±8 ppmv	145 ppmv
NO_x	±0.25 ppmv	34 ppmv
NO_2	±0.25 ppmv	26 ppmv

TABLE V
RESPONSE RATES OF THE MEASUREMENT SYSTEM

Species	Response Rate[1], sec	
	Instrument Alone	Measurement System
CO	3	10
CO_2	3	10
C_xH_y	6	15
NO_x	200	206
NO_2	220	226

[1]Time required to attain 90 percent of the steady-state value, measured from application of calibration gas.

TABLE VI
GASEOUS EMISSIONS RATES AT THE NOZZLE EXIT

Species	CO			C_xH_y			CO_2			NO_2			NO_x		
Power Level	lbm/sec	lbm/lbm	lbm/lbf hr	lbm/sec	lbm/lbm	lbm/lbf hr	lbm/sec	lbm/lbm	lbm/lbf hr	lbm/sec	lbm/lbm	lbm/lbf hr	lbm/sec	lbm/lbm	lbm/lbf/hr
Idle	0.027	0.15	1.32	0.0076	0.042	0.37	0.51	2.82	25.0	0.00055	0.0031	0.027	0.00095	0.0053	0.046
Cruise	0.029	0.058	0.072	0.0047	0.0094	0.012	1.82	3.65	4.53	0.0020	0.0040	0.0049	0.0018	0.0036	0.0042
Military	0.034	0.046	0.050	0.0043	0.0058	0.0063	2.56	3.54	3.76	0.0028	0.0039	0.0041	0.0040	0.0054	0.0056
Minimum Afterburning	0.087	0.086	0.114	0.088	0.087	0.115	3.25	3.25	4.26	0.0034	0.0034	0.0044	0.0091	0.0090	0.0119
Mid-Afterburning	0.060	0.038	0 0 69	0.016	0.0102	0.018	5.22	3.36	5.99	0.0024	0.0016	0.0028	---	---	---
Maximum Afterburning	0 066	0.035	0.064	0.0075	0.0040	0.0073	5.62	3.02	5.50	0.0029	0 0015	0.0028	0.0057	0.0031	0.0056

lbm emission/hr/lbf thrust
lbm emission/lbm fuel
lbm emission/sec

UNCLASSIFIED
Security Classification

DOCUMENT CONTROL DATA - R & D

(Security classification of title, body of abstract and indexing annotation must be entered when the overall report is classified)

1. ORIGINATING ACTIVITY (Corporate author)
Arnold Engineering Development Center,
Arnold Air Force Station, Tennessee 37389.

2a. REPORT SECURITY CLASSIFICATION
UNCLASSIFIED

2b. GROUP
N/A

3. REPORT TITLE
MEASUREMENT OF POLLUTANT EMISSIONS FROM AN AFTERBURNING TURBOJET ENGINE AT GROUND LEVEL II. GASEOUS EMISSIONS

4. DESCRIPTIVE NOTES (Type of report and inclusive dates)
June 22 thruogh September 21, 1971--Final Report

5. AUTHOR(S) (First name, middle initial, last name)
G. R. Lazalier and J. W. Gearhart, ARO, Inc.

6. REPORT DATE	7a. TOTAL NO. OF PAGES	7b. NO. OF REFS
August 1972	63	9

8a. CONTRACT OR GRANT NO.

b. PROJECT NO. 3066

c. Program Element 62203F

d. Task 05

9a. ORIGINATOR'S REPORT NUMBER(S)
AEDC-TR-72-70

9b. OTHER REPORT NO(S) (Any other numbers that may be assigned this report)
ARO-ETF-TR-72-30

10. DISTRIBUTION STATEMENT
Approved for public release; distribution unlimited.

11. SUPPLEMENTARY NOTES
Available in DDC.

12. SPONSORING MILITARY ACTIVITY
AFAPL (TBC)
Wright-Patterson Air Force Base
Ohio 45433

13. ABSTRACT
The performance of a sampling and measurement system for the gaseous species of carbon monoxide (CO), carbon dioxide (CO_2), total hydrocarbons (C_xH_y), nitrogen dioxide (NO_2), and total oxides of nitroge (NO_x) was demonstrated for engine power conditions from idle to maximum afterburning at ground level. Data were obtained, using a protable emissions measurement system developed at AEDC, at positions ranging from immediately at the nozzle exit to 96 ft aft of the nozzle exit plane. A J85-GE-5 engine was used to generate the gaseous emissions. Nondispersive infrared detectors were used for CO and CO_2 measurements; a flame ionization detector was used for C_xH_y measurements; and electrochemical devices operating on the fuel cell principle were used for NO_2 and NO_x measurements. The effects of inlet humidity and crosswind velocity on the quantity and distribution of gaseous species in the exhaust plume were determined.

DD FORM 1 NOV 65 1473

UNCLASSIFIED
Security Classification

14. KEY WORDS	LINK A		LINK B		LINK C	
	ROLE	WT	ROLE	WT	ROLE	WT
air pollution						
contaminants						
turbojet engines						
gases						
emission						
exhaust gases						
exhaust emissions						
afterburner						

AFSC
Arnold AFS Tenn.